THE PENNSYLVANIA STATE UNIVERSITY
SCHREYER HONORS COLLEGE

DEPARTMENT OF BIOMEDICAL ENGINEERING

AN INVESTIGATION INTO THE NANOFIBER-INDUCED EPIGENETIC CHANGES IN MESENCHYMAL STEM CELLS

MATTHEW DAVID SWATSKI
SPRING 2016

A thesis
submitted in partial fulfillment
of the requirements
for a baccalaureate degree
in Biomedical Engineering
with honors in Biomedical Engineering

Reviewed and approved* by the following:

Justin L. Brown
Assistant Professor of Biomedical Engineering
Thesis Supervisor

William O. Hancock
Professor of Biomedical Engineering
Honors Adviser

Dr. Jian Yang
Professor of Biomedical Engineering
Faculty Reader

* Signatures are on file in the Schreyer Honors College.

ABSTRACT

Substrates, such as microgrooves and nanofibers that attempt to mimic the extracellular matrix, have been shown to direct the differentiation of mesenchymal stem cells (MSC). The shape, aspect ratio, and curvature of the substrate are all factors that can direct MSC differentiation toward a specific lineage. The diameters of the nanofibers have been shown to play a role in directing differentiation. However, the mechanism by which this occurs is still unclear. This study proposes that one of these mechanisms is the epigenetic modification of the histone H3 protein. The acetylation of the histone H3 protein expedites transcription of the DNA, while methylation may turn specific genes “on” or “off”. In this study, mesenchymal stem cells are seeded onto PMMA nanofibers, and the epigenetic proteins of dimethylated H3 K9, dimethylated H3 K4, acetylated H3 K9/K14, total acetylated H3, and Erk1/2 were examined. The PMMA Nanofibers were created by electrospinning a solution of 30% m/v PMMA in nitromethane onto a T-Glase scaffold. The fibers are relatively aligned and their diameter is approximately 3.38 ± 0.53 μm. There was a statistically significant decrease in the dimethylated H3 K9, the dimethylated H3 K4, and Erk1/2 expression. There was a significantly increase in the total acetylated H3. The changes in these epigenetic proteins point to a signaling response that is caused by the cells interacting with nanofiber scaffolds. The investigations also examined whether these epigenetic responses are heritable. The cells were found to maintain some of these modifications following removal from the PMMA nanofibers and placement onto a flat control surface.

TABLE OF CONTENTS

LIST OF FIGURES

LIST OF TABLES

ACKNOWLEDGEMENTS

These past three years in Dr. Brown's lab have been a time of immense growth and intellectual stimulation. I was challenged by the work, and it required me to become a more organized, efficient student and engineer. There is no doubt in my mind that I would have given up and not completed this project if it weren't for the near-infinite patience of Dr. Brown, the graduate students, and the other undergraduates. Dr. Brown is an incredible mentor, and I am truly honored to have had the opportunity to work in his lab. He has allowed me to make mistakes and grow into a better researcher and student. I am thankful that he didn't ever get frustrated with the difficulties that I encountered. He was always able to be a helpful guide in all of my lab work. Almost as important as Dr. Brown was Brittany Banik. Brittany faced the brunt of my questions, messes, and difficulties. She is an incredible teacher, and the lab is extremely lucky to have her as a stabilizing force. If it weren't for Dr. Brown and Brittany, I probably would not be graduating as a Biomedical Engineer.

The presence of Dan Bowers in the lab has been immensely helpful as well. It is hard to quantify how many answers, tips, and advice he provided to me during the past 18 months in the lab. He is extremely creative, and much of the progress in the project is due to his ideas and suggestions. If it weren't for Dan, I do not think that I would have anything to show after three years. There have also been many others in the lab over the past three years who have given advice and tips. If it weren't for their small pieces of advice and assistance, I don't think I would be here today. Richard Karp, Christina Platt, Dan Cognetti, and Tom Riley all were extremely helpful during my sophomore year when I was just beginning this project. They all worked along aside me to make this succeed. Mary Elizabeth McCulloch and Rebecca Nagurney

have given immense help to remind me to complete parts of this Thesis at the deadlines. Finally, Pouria Fattahi, Jen Madary, Rachel Wolfe, Harvey Li, and Jordan Dover have all given tips and advice throughout the past two years that have helped me succeed.

Finally, I would like to thank my parents who gave me the opportunity to attend Penn State. They have been extremely patient during my summers in State College trying to conduct the experiments just one more time (because **this time**, I told them, it will work).

Chapter 1

Introduction

Over 2 million Americans each year require procedures to repair and reconstruct damaged bone, muscle, joints, and ligaments (Ozdemir, Higgins, & Brown, 2015). Researchers in the field of regenerative medicine seek to heal or replace damaged tissues. This is done through the use of stem cells, biomaterials, and/or growth factors. Stem cells have a unique ability to differentiate into any of the 200 unique cell types found in the human body. Therefore, they have the capacity to create new human tissues or organs that can be implanted into patients. Regenerative medicine is a burgeoning field that merges materials engineering with biological systems to improve or replace living tissue. In a conventional regenerative medicine project, scaffolds of biomaterials are constructed, stem cells are placed onto the scaffolds with bioactive growth factors, and the scaffolds are then placed into a bioreactor to promote tissue growth. These growth factors, such as bone morphogenetic proteins (BMP) and epidermal growth factor (EGF), promote differentiation of stem cells towards specific lineages (Linkhart, Mohan, & Baylink, 1996) (Carpenter & Cohen, n.d.). Recent advances in stem cell research and biomaterials have allowed for the creation of many types of artificial tissues and organs, such as bladders, pancreas, and cartilage. More ambitious projects, such as the creation of hearts, livers, and kidneys are currently underway.

High concentrations of growth factors have been shown to direct the differentiation of mesenchymal stem cells (MSCs), but they are prohibitively expensive to be effective therapeutically. However, recent studies have found that the substrate onto which the

cells are plated can also direct differentiation. Substrates, such as microgrooves and nanofibers, attempt to mimic the extracellular matrix (ECM) (Downing et al., 2013a). The shape, aspect ratio, and curvature of the substrate are all factors that can direct MSC differentiation toward a specific lineage (Kai, Jin, Prabhakaran, & Ramakrishna, 2013).

History of Regenerative Medicine

The fields of tissue engineering and regenerative medicine have experienced a surge in the last 30 years due to advancements in the fields of materials science, microbiology, and microscopy. This convergence of disciplines has led to the prediction of the revolutionary nature of tissue engineering. Although the field has not been as revolutionary as predicted, there have been successes in the creation and healing of damaged or articifical tissues. The first account of organ regeneration dates back to ancient Greek myths, when Prometheus' liver was eaten by an eagle each night, but would grow back each day. Later stories tell of the Christian Saints, Cosmas and Damien, who miraculously attached the leg of a cadaver to a patient with an ulcerated leg. In the 19th century after the advent of modern medicine, came the first skin grafts, corneal transplants, and autologous bone grafts. Even today, the autologous bone graft is the "gold standard" of tissue enginering (Sen & Miclau, 2007). During an autologous bone graft, bone is taken from one part of the body, usually the iliac crest, and transplanted to a region of damaged bone.

There are examples in nature of the regrowth of damaged or diseases tissue without the use of artifical scaffolds or treatment. The most impressive is that of the salamander. Within salamander limbs, there is a population of mesenchymal stem cell satellite cells. These

satellite cells give salamanders the ability to regrow limbs or parts of limbs (Morrison, Lööf, He, & Simon, 2006). Mammals do not have this satellite cell population, and therefore, cannot regrow complex organs and tissue. Another example in nature of partial tissue regeneration is the human liver. All mature liver cells participate in this extremely complex process by which hepatocytes can regrow removed or damaged portions of the liver to its original state (Michalopoulos, 2007). Also, the endometrium within the human uterus regrows after every menstrual cycle. It is the only tissue within the human body to regrow following complete breakdown.

Although there are examples of tisue regeneration in nature, this is not possible for the vast majority of human tissues. The field of tissue engineering has been defined as the application of biomaterials, growth factors and cells either alone or in combination towards the generation or regeneration of damaged and diseased tissues and organs. The coordination of biomaterials, growth factors, and cells allows engineers to attempt to design nearly every organ in the human body.

Tissue engineering had its earliest beginnings in the 1980s with the isolation of embryonic stem cells from mice in 1981. Embryonic stem cells are defined their ability for unlimited proliferation, differentiation to all tissue types except the placenta, and participation in all three germ layers in a chimera. These mice embryonic stem cells, when cultured with mouse fibroblasts, were able to differentiate into teratocarcinomas, which are tumors that contain cells from all three germ layers. The presence of cells from all three germ layers proves the pluripotency of embryonic stem cells. Also, it shows that there was a growth factor being expressed by the fibroblasts that caused the embryonic stem cells to differentiate. The next breakthrough study occurred in the 1983, with the reconstitution of living skin by placing

fibroblasts, which are connective cell precursors, in a collagen gel that mimics the ECM. Following that, keratinocytes were seeded on top of the fibroblasts. These two cell layers allowed for the creation of the epidermis on top of the dermis layer (Bell et al., 1983).

The first example of cell culture on an artificial "ECM" was completed in 1988 with the transplantation of hepatocytes onto a Polyglactin 910 (Vacanti et al., 1988). The polymer Polyglactin 910 is a biocompatible, common polymer used in surgical sutures. To further expedite the need for extracellular scaffolds, human mesenchymal stem cells (hMSCs) were shown to differentiate into bone cells if they were allowed to spread, or fat cells if they were rounded. There was also evidence that the RhoA:ROCK signaling activity plays a role in orchestrating the differentiation, along with cytoskeletal tension (McBeath, Pirone, Nelson, Bhadriraju, & Chen, 2004). The next breakthrough with artificial ECMs occurred in 2006 with the creation of an artificial bladder. Urothelial and muscle cells taken from a patient during a biopsy were seeded onto an artificial scaffold made of collagen and polyglycolic acid (PGA). This autologous bladder was then implanted into the patient, and function returned to normal (Atala, Bauer, Soker, Yoo, & Retik, 2006). Another strategy involving the use of ECMs involved the use of decellularized organs. In 2008, researchers published a study where a rat's heart was decellularized, leaving only the ECM structure. Then, the heart was injected with endothelial cells and cardiomyocytes, and perfused in a bioreactor for 28 days. Under electrical stimulation, the heart began to beat and pump saline solution, but the pump function was only 2% of that of the average working heart (Ott et al., 2008). Again in 2008, a fascinating scaffold was made that attempted to model cardiac anisotropy. An accordion-like honeycomb structure was made to mimic the fact that different mechanical properties of the heart exist depending on whether the stress occurs in the vertical or horizontal directions. Small channels were created within the

honeycomb structure to allow the cardiac signal pulse to propagate through the cardiomyocyte tissue (Engelmayr et al., 2008). Also in 2008, an artificial trachea was constructed for a woman with a severely constricted trachea by a bacterial infection. A cadaver's trachea was decellularized, and then the patients' chondrocytes and epithelial cells were placed in a rotating bioreactor along with the decellularized trachea. The new trachea was then implanted into the same location as the infected trachea, and the "graft immediately provided the recipient with a functional airway, improved her quality of life, and had a normal appearance and mechanical properties at 4 months." (Macchiarini et al., 2008).

There have also been many attempts to create artificial blood vessels, which are the "Holy Grail of peripheral vascular surgery" (Kakisis, Liapis, Breuer, & Sumpio, 2005). Since all tissue needs perfusion, developing artificial blood vessels can help engineers create more complex organs that require regular blood supply. In the late 1980s and early 1990s, there were attempts made to create artificial vasculature with both Type I and Type III collagen, but the mechanical properties of these grafts was poor. Type I collagen is typically present in scar tissue, while Type III collagen is found in bone, cartilage, tendon, and other connective tissue. One group used a Dacron mesh to reinforce the Type I collagen scaffold, but they were able to seed canine jugular smooth muscle cells and endothelial cells onto this scaffold to create a graft that had a patency of 65% after 6 months when implanted into the Canine posterior vena cava (Hirai, Kanda, Oka, & Matsuda; Hirai & Matsuda). Eventually, in the 1990s and the 2000s, researchers began to use synthetic biodegradable polymers, such as PGA, polyhydroxyalkanoate (PHA), caprolactone (CL), and lactic acid (LA) for their scaffolds. Two groups were able to achieve 100% patency with their PGA-PHA and PGA-CL/LA vascular grafts. One group used ovine smooth muscle cells, endothelial cells, and fibroblasts with a PGA-PHA graft, and implanted it

into an ovine infrarenal aorta. This was 100% patent after 5 months (Shum-Tim et al., 1999). The second group used canine smooth muscle cells and fibroblasts with PGA-CL/LA graft, and implanted it into a canine inferior vena cava. This was also 100% patent even after 13 months (Watanabe et al., 2001).

Another popular field of research in tissue engineering is Anterior cruciate ligament (ACL) reconstruction. This is one of the most frequently injured ligaments in the knee, and there is much research dedicated toward repairs and prosthetics for the ACL (Mascarenhas & MacDonald, 2008). One group used poly-L-lactic acid (PLA), and poly(DTE carbonate) to create scaffolds. The PLA scaffold could not withstand the mechanical strength required, but the poly(DTE carbonate) graft, when seeded with fibroblasts, had an ultimate tensile strength similar to that of an ACL. A second group examined two different types of collagen-scaffold cross-linking, ultraviolet irradiation (UV) or 1-ethyl-3-(3-dimethylaminopropyl) carbodiimide (EDC). Although seeded fibroblasts proliferated quicker in the UV cross-linked collagen, the EDC cross-linked collagen had better mechanical properties. Therefore, the EDC cross-linked collagen scaffold was superior to the UV cross-linked collagen scaffold, because the EDC cross-linked collagen scaffolds just required a longer culturing period (Caruso & Dunn, 2005). A third research group explored the use of growth factors on rabbit ACL. It was found that the addition of basic fibroblast growth factor, transforming growth factor-β1, bone insulin, and platelet-derived growth factor-β1 in combination increased cell growth by 20-30 times (J. Lee, Green, & Amiel, 1995). A fourth research group investigated the optimal dosing concentrations to encourage cellular proliferation and tissue growth (Murray & Rice, 2003). The difficulty with using growth factors *in vivo* is that they can are degraded quickly by enzymes, therefore they have extremely limited use.

Stem Cells

The term “stem cells” denotes a large class of cells that can differentiate into all, a few, or even just one cell type. **Figure 1** gives a snapshot of the myriad of lineages that the cells can proceed down. The term “potency” is used to describe how many cell types any given stem cell can differentiate into. For example, when an egg is fertilized, the single-celled zygote is totipotent. Therefore, this cell can become any of the three germ layers and the placenta. If a totipotent cell were to be separated from the organism, it may grow into its own separate human life. After several divisions, the cells of the morula lose this totipotent ability. These cells are now a part of the blastocyst. The blastocyst has an outer layer of cells, known as the trophoblast, that will eventually become the placenta. In the inner cell mass of the blastocyst are cells known as embryonic stem cells (ESCs). These embryonic stem cells have the potential to become any cell of any of the germ layers in the human body, with the exception of cells in the placenta. Once an embryonic stem cell “chooses” to become one of the germ layers, its descendants cannot revert back to its embryonic state and become a different germ layer.

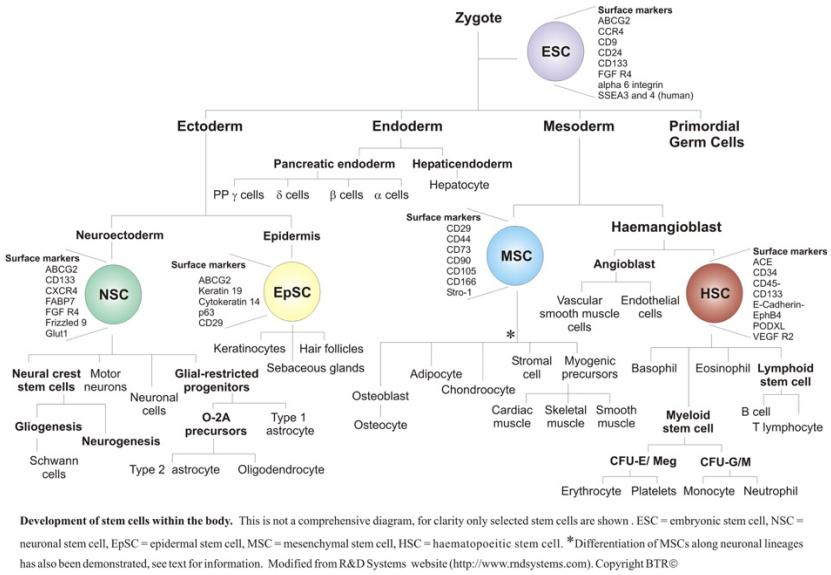

Development of stem cells within the body. This is not a comprehensive diagram, for clarity only selected stem cells are shown . ESC = embryonic stem cell, NSC = neuronal stem cell, EpSC = epidermal stem cell, MSC = mesenchymal stem cell, HSC = haematopoeitic stem cell. *Differentiation of MSCs along neuronal lineages has also been demonstrated, see text for information. Modified from R&D Systems website (http://www.rndsystems.com). Copyright BTR©

Figure 1: The differentiation potential of ESCs. (http://www.york.ac.uk/res/bonefromblood/background/osteogenesis.html.)

After an embryonic stem cell journeys down a germ layer path, the DNA of its offspring becomes more modified, and their potential functions become more restricted. Eventually, an embryonic stem cell's descendants will reach the adult stem cell stage. Adult stem cells are present in all three germ layers, and they act as a reserve to replace damaged or diseased tissue of that germ layer. Adult stem cells can either replicate into more adult stem cells, or they can differentiate and choose an even more specific lineage. The latter of these cells will eventually become adult or somatic cells. Eventually, as more physical and chemical environmental factors modify and direct the cell, they lose their ability to differentiate. These somatic cells may divide, but they will not differentiate further into any more specialized lineages. In this investigation, mesenchymal stem cells (MSCs) are experimented on. Mesenchymal stem cells are adult, multipotent stem cells that can differentiate into many types of tissue found within the mesoderm germ layer, such as osteoblasts, tenocytes, and myoblasts. **Figure 2** shows the adult stem cells that MSCs can become. They are typically found in umbilical cord tissue, amniotic fluid, molars, and especially bone marrow.

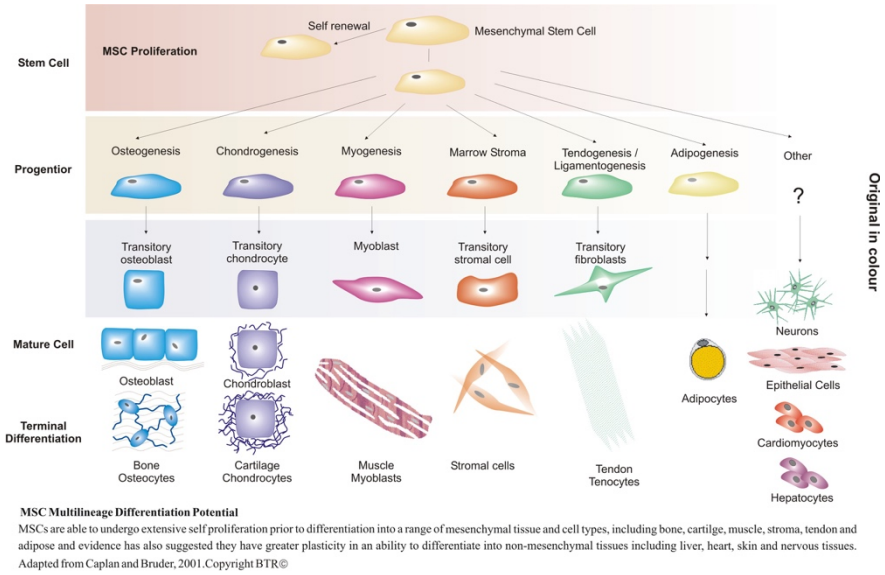

Figure 2: The differentiation potential of MSCs into their many lineages. (http://www.york.ac.uk/res/bonefromblood/background/osteogenesis.html.)

The creation of induced pluripotent stem cells (iPSCs) was a revolutionary step forward in the understanding and production of stem cells. It had been known for several years with the fame of Dolly the Sheep in 2003, that nuclei from a somatic cell could be implanted into an unfertilized oocyte, and then be coerced into growing into a blastocyst and eventually, an adult organism. However, this method has ethical questions surrounding it with regards to human use, and there hasn't been much success in humans. In 2006, researchers discovered that only only four genes were required to the reversal of a somatic cell to its pluripotent state. These genes coded for the transcription factors, Oct3/4, Sox2, c-Myc, and Klf4. These induced pluripotent stem cells (iPSCs) were able to be become all three germ layers when placed into mouse blastocysts, which proves that they function like embryonic stem cells. (Takahashi & Yamanaka, 2006). Then, in 2013, researchers were able to dervice iPSCs directly from MEFs using only a combination of seven small molecules (Hou *et al.*, 2013). This allows iPSCs to be derived without exogenous expression of genes that were inserted into the nucleus virally, or by

somatic cell nuclear transfer from an oocyte. In 2014, a Japanese woman was the first to ever have her own cells brought back to the pluripotent state. These iPSCs were then grown into a retinal sheet and implanted into her eye to treat macular degeneration (Cyranoski, 2014).

Scaffold-Creation Methods

When choosing a type of scaffold, there are several types of controllable parameters of the scaffold that must be taken in to consideration before designing and creating such a structure. Before considering these parameters, it is appropriate to look at the five different functions of ECM, which is what the scaffold is attempting to mimic (Chan & Leong, 2008). First, the ECM has to be conducive to cell growth. It must provide the structural support and space to be able to attach, grow, migrate, divide, and respond to inter-cell signaling. Second, the ECM must provide a similar the mechanical rigidity and elasticity as that of the host tissue. Third, the ECM must be able to have bioactive cues that regulate the cells and its function. For example, RGD peptides on fibronectin have been shown to promote cell adhesion (Hersel, Dahmen, & Kessler, 2003). Fourth, the ECM may have embedded growth factors to promote tissue growth and cell proliferation. Fifth, the ECM must degrade to allow for vascular remodeling and wound healing. There are many morphological changes during the life of any given tissue, and the ECM has to be able to respond to them properly.

For all of these functions of the ECM, most scaffolds will want to have many or all of these functions, depending on the tissue need. The scaffold must be porous enough to allow cells to attach, migrate, and proliferate. For all complex tissue structures and organs, vascularization is necessary for growth. Therefore, the scaffold must be designed to encourage

angiogenesis and allow for the vascularization of the interior. However, the scaffold cannot be so porous that it will compromise its mechanical integrity. Finding the proper material and 3D shape is critical to maintaining mechanics of the scaffold. Also, the material must be biocompatible with cell attachment, and it should not trigger an immune response from the endogenous tissue. Depending on the environment, the scaffold may also want to release biomolecules following its swelling or degradation. This can induce cells placed on it to perform a specific function or differentiate. Related to this release of biomolecules, it must be considered the rate of degradation for this scaffold. The rate at which the newly-built ECM grows may determine the speed at which the artificial scaffold degrades. Also important is the chemical or physical byproducts of the degradation of the scaffold material. Any toxic or immunogenic materials must be avoided. Finally, the force applied to the scaffold and the stiffness of the substrate can induce stem cells to differentiate toward one lineage or another. For example, pliable matrices are neurogenic, stiffer matrices are myogenic, and hard matrices are osteogenic (Engler, Sen, Sweeney, & Discher, 2006). This exactly mimics the external environment in these tissues.

There have been three different types of techniques toward the creation of scaffolds. In the first method, the scaffold material is dissolved in a solvent. A porogen made of liquid, gas, or small molecule is added to this solution as well. Then, the solvent is evaporated, melted, or sublimated. This way, what is left is the scaffold filled with the porogen within the pores. If the porogen is solid, it is then dissolved away with another solvent that doesn't dissolve the scaffold. The amount, size, shape, and interconnectivity of the pores can all be optimized to create the desired scaffold parameters (Chevalier & Chulia, 2008). In the second method, scaffolds are created by selective laser sintering, stereolithography, and 3D printing. Selective laser sintering

is when a laser fuses two materials together, and this allows the computer to build a complex, hierarchical structure out of a powder. Another type of additive manufacturing is known as stereolithography, which uses UV light to draw an outline from a computer into a mold. The UV light causes the resin material to harden, leaving a hierarchical structure as each layer is hit with the UV light. Stereolithography has been used to create hydrogels onto which cells are seeded (Dhariwala, Hunt, & Boland, 2004). 3D printing is the third type of additive manufacturing that uses a computerized extruder to lay down layers of hot plastic that will solidify to become a solid material. This is one of the two methods used in this study. The third method for scaffold design, and the method that is used in this study, is electrospinning.

Nanofibers

To understand how to modify nanofibers, the theory of nanofibers has to be understood first. The creation of nanofibers is done primarily through electrospinning. A diagram of electrospinning is shown in **Figure 3**. During electrospinning, the nanofibers are created by ejecting a polymer solution from a syringe across an electric field. As the solvent evaporates, the polymer attaches to either a two-dimensional hydrogel or a three-dimensional scaffold, forming fibers between several nanometers to two micrometers.

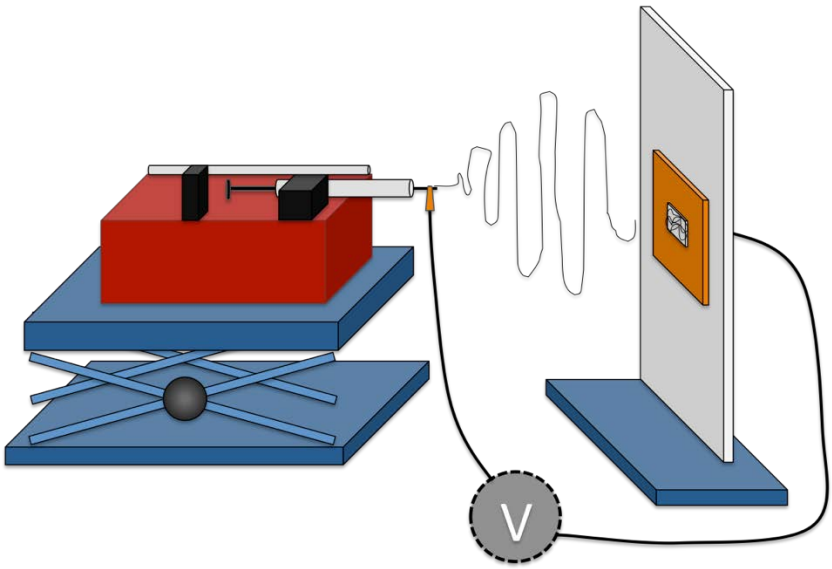

Figure 3: Diagram of Electrospinning (Photograph Courtesy of Brittany Banik)

The parameters of the nanofibers, such as density, diameter, and alignment, can be optimized to simulate various conditions within living tissues. Other material properties such as the stability and functional groups of the polymer may also be modified to achieve different material conditions.

As the solution exits a needle, it forms a cone that is being pulled by the electric field. This cone is known as the Taylor cone. Depending on the conductivity of the solution, the polymer will begin to be pulled at a certain height of the Taylor cone. The radial charge repulsions cause the polymer to divide into polymer strands of approximately equal diameter. As the polymer begins to spray, it begins to whip at high frequency in a phenomenon known as splaying. Splaying is what allows the polymer to break into equal-diameter strands. The final diameter of the nanofibers depends on the amount of whipping action that was able to break up the polymer strand (Reneker & Chun, 1996). The collection region is when the whipping action of the nanofibers has stopped, and the nanofiber has reached its final diameter. In the case of this

project, the nanofiber collects onto the T-Glase Scaffold Grid or coverslip taped to the back of the metal plate in the electrospinning apparatus.

Nanofibers have had many potential uses in the field of regenerative medicine. In Dr. Justin Brown's lab, Ph.D. Candidate Brittany Banik is using nanofibers to construct an artificial tendon that. Another excellent example of how structure of the scaffold affects the function is that of the recreation of the annulus fibrosus, or the exterior of the vertebral disks, through MSC seeding onto nanofibers. The different layers of fibers alternated by 30° both above and below the transverse plane. This alternating fiber alignment mimics collagen fiber alignment present in the annulus fibrosus. This multi-level, alternating angle structure achieved physiological mechanical structure by 10 weeks of *in vitro* culture with MSCs. No previous study that failed to take into account the complex mechanical architecture successfully led to the growth of new annulus fibrosus (Nerurkar et al., 2009).

Nanofibers have also been implicated in the conduction of cardiac signals even through alginate gels (Dvir, Timko, & Brigham, 2011). Cardiac patches are small patches of heart tissue that can be used in replacing damaged cardiac tissue. Cardiac cells have been successfully grown in alginate gels, which has has been approved for phase II clinical trials for treating myocardial infarction. However, these alginate gels have poor conductivity. When gold nanowires, each with a diameter of approximately 30 nm and a length of approximately 1 μm, were incorporated into the alginate gel, the cardiomyocytes and fibroblasts that were seeded were thicker, better aligned, and most importantly, showed a synchronized electrical conductivity. These nanofibers are expected to improve the quality of cardiac patches.

There is also myriad of polymers that can be used in electrospinning. Biopolymers are one class of polymers that are extracted from the natural environment through sources such as

crustacean shells, mushrooms, wood, and silk worms. Cellulose, chitin, chitosan, dextrose, collagen, gelatin, and silk are some examples of biopolymers that can be derived from these natural sources (Schiffman & Schauer, 2008). There is a nearly infinite combination of potential polymer solute-solvent mixtures. Some of the more popular polymers for biomedical applications include poly(methyl methacrylate) (PMMA), polycaprolactone (PCL), poly(lactic-co-glycolic acid) (PLGA), poly(vinyl alcohol) (PVA), and poly(ethylene glycol) (PEG). Popular solvents for electrospinning are tetrahydrofuran (THF), nitromethane, 2,5-dimethylfuran (DMF), dichloromethane (DCM), acetone, ethanol, and distilled water. The combinations of these solutes and solvents produce nanofibers with different properties. Even the combination of solvents can also create nanofibers with unexpected results. For example, mixtures of the solvents DMF/THF cause autoflourescence of the nanofibers, which prevents them from being observed under a flouresecent microscope. Three-dimensional scaffolds of nanofibers are used extensively in regenerative medicine, because artificial tissues are grown on them.

In this project, there are many aspects of the electrospinning process that can be modified to produce various types of fibers. For example, changing the solution concentration can produce beaded and changing the distance of the electric field (or the distance from the syringe tip to the metal plate) can affect the size of the fibers. This is because there was not enough splaying while the polymer was moving through the electric field. Adding magnets to the metal plates can alter the whipping motion, and fibers can be produced to align with the magnetic field that is created by the magnets. Finally, even the humidity can affect the consistency of the fibers. A more humid atmosphere within the electrospinning apparatus produced fibers that do not stick the surface, because of increased water adsorption to the coverslip and metal plate.

ECM-Directed Differentiation and Cell-Signaling Pathways

When a cell lands on a substrate, the focal adhesions of the cell allow it to attach to the surface on which it has landed. Focal adhesions are an assembly of nearly 150 proteins between that act as the bridge between the ECM and the actin fibers of the cytoskeleton (Zaidel-Bar & Geiger, 2010). Integrins are proteins that allow the cell to attach to the ECM, and they are responsible for the transmitting the mechanically-induced signals in to the cell from the ECM. There is evidence that RhoA:ROCK:Myosin II signaling pathway and FAK:ERK1/2:Runx2/Cbfa-1 signaling pathway are implicated in osteogenic differentiation (Ozdemir et al., 2015) (Salasznyk, Klees, Williams, Boskey, & Plopper, 2007) through integrin-mediated mechanosensing. In the case of Ozdemir et al. this mechanical direction of osteogenic, chondrogenic, and adipogenic differentiation has been shown to occur due to PMMA nanofibers of varying sizes. The size ranges of the nanofibers are less than that of this study. In Ozdemir et al. the size of the nanofibers are from 0.2 – 1.5 μm, while in this study the nanofiber diameter is approximately 3.38 ± 0.53 μm. **Figure 4** shows the normalized differentiation of MSCs to either an adipogenic, chondrogenic, or osteogenic lineage as a function of the nanofiber diameter.

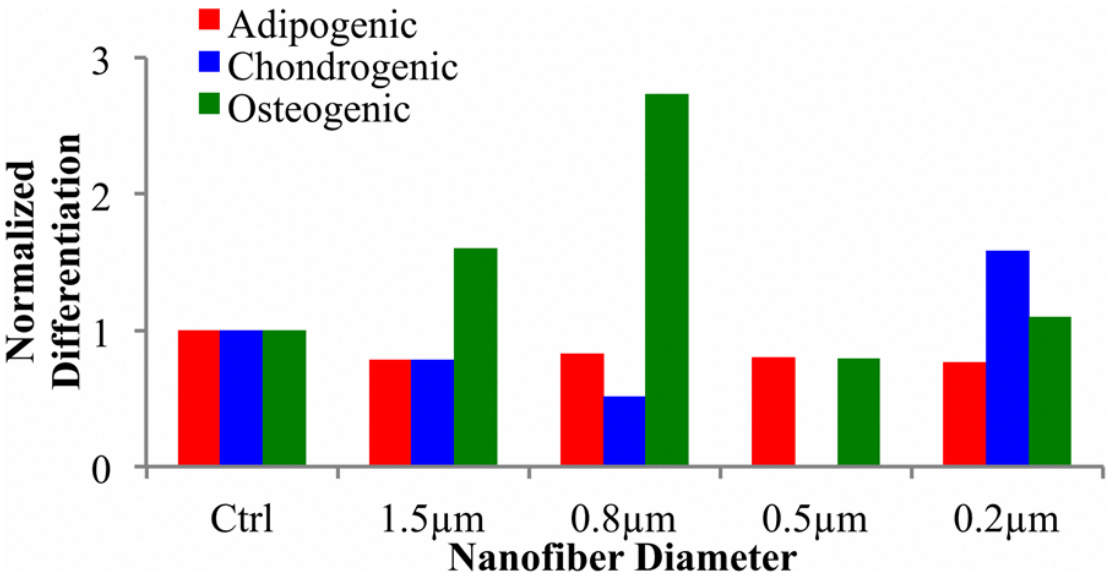

Figure 4: Normalized Differentiation as a Function of Nanofiber Diameter (Ozdemir et al., 2015)

There have been studies that have implicated fibers closer in size to the ones examined in this study. One study found that 0.5 – 2.5 µm PMMA nanofibers all showed a significant decrease in JNK, and an increase in ERK and p38 signaling. There have been experiments with several substrate topologies such as grooves, pits, and pillars confirm that integrin-mediated mechanosensing of these environment can activate ERK1/2 and p38 (Boutahar, Guignandon, Vico, & Lafage-Proust, 2004). ERK1/2, p38, and JNK are all involved in the MAPK signaling pathway, that modulates cell proliferation and differentiation.

Epigenetics

Since all cells have the same DNA sequence, yet perform different functions, the cell must have mechanisms by which it preserves its function and identity during cell division. These mechanisms include small interfering RNAs (siRNAs), DNA methylation, histone variants, and post-translational histone modifications, and collectively are known as epigenetics. Epigenetics

is defined as the “the stable and heritable information that is distinct from DNA sequences and fostered by specialized mechanisms” (Margueron & Reinberg, 2010). DNA methylation and some post-translational modifications have been shown to be heritable between somatic cells, it is suspected that post-translational modifications play a large role in transmitting the epigenetic information from parent cell to daughter cell (Wigler, Levy, & Perucho, 1981) (Gaydos, Wang, & Strome, 2014). Part of this study attemps to determine the heritability of epigenetic changes following removal from the nanofiber substrates and subsequent cell divisions.

In this study, the post-translational modifications of the H3 protein are examined. There is no current research that confirms that H3 modifications are heritable. In the cell, the chromatin is condensed around histones. These histone proteins are made of four different quadrants (H1 H2A/B, H3, H3) each of which can have some their amino acids modified (typically lysinse, serine, or arginine) to allow for a change in the way the chromatin is wound around the histones. Analogously, the “tighter” the winding of the chromatin around the histone, the less likely the chromatin will be transcribed, and the more “loosely” the chromatin is wound, the more likely it will be transcribed. **Figure 5** shows the histone proteins and the complex relationships between them, transcription factors, and the final somatic stage. **Figure 5** also shows the various function groups which can be covalently modified to lead to the final adult cells.

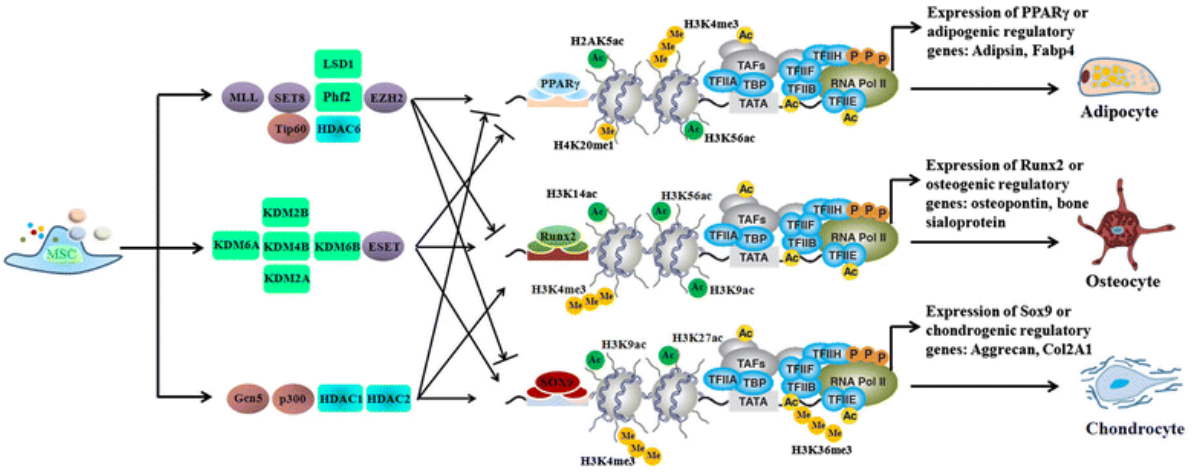

Figure 5: Pathways to cellular differentiation (Huang, Li, & Jiang, 2015)

It has been previously shown that dimethylated H3 K9 promotes chondrogenesis and adipogenesis and inhibits osteogenesis, dimethylated H3 K4 promotes adipogenesis and inhibits osteo/dentingenesis, acetylated H3 K9/K14 modulates osteogenesis and inhibits adipogenesis and cardiomyogenesis, and Erk1/2 has been show to decrease with larger nanofibers and directed osteogenic differentiation (Huang et al., 2015) (Jaiswal & Brown, 2012). Therefore, with large nanofibers (> 0.8 μm) , it is expected to have a statistically significant decrease in the expression of all these proteins when placed on 3.38 ± 0.53 μm PMMA nanofibers as compared to a flat, polystyrene control surface. The protein expression has been evaluated by immunofluorescence, an in-cell western blot, and western blots.

Chapter 2

Methods

Cell Culture

Although there was much variation in the experiments that were conducted, the type of cells that were used remained relatively constant. From the beginning of the experiments, mouse mesenchymal stem cells (MSCs) were used. These MSCs were obtained from GIBCO. MSCs lived in alpha-modified minimum essential medium (α-MEM) at approximately 0.5 mL/cm^2. The α-MEM had added 10% fetal bovine serum (FBS) from Atlanta Biologicals and 1% (vol/vol) penicillin/streptomycin (Pen/Strep) from Lonza. During cell culture, there was approximately 2 mL of media per 6-well plate and 20 mL of media per 145 mm x 20 mm Greiner CELLSTAR® dish. However, when the cells were seeded onto the T-Glase scaffolds with PMMA nanofibers, 4 mL of α-MEM would be used. Every two days, the cell media would be changed.

Throughout most of the experiments, the MSCs have always been Passage 9 or greater. A Passage is defined as when the MSCs are 60-70% confluent on a 145 mm x 20 mm Greiner CELLSTAR® dish. Passage they reached during experiments was Passage 17. For all of the final western blot results, the MSCS never grew above Passage 10. The cells were cultured in a humidified incubator (Nuaire Autoflow IR Direct Heat CO_2 incubator) at 37 °C with 5% CO_2.

The MSCs were first thawed from cryostorage from an LS-750 Taylow-Wharton Lab Systems liquid nitrogen tank. The cells were at -200 °C after being frozen previously. 18 mL of α-MEM was added to the approximately 2 mL of frozen MSCs.

After the cells reached 60-70% confluency, cell passage was performed. Cell passage was performed in a NUAIRE LABGARD ES Class II, Type A2, Biological Safety Cabinet. The media was aspirated from the 145 mm x 20 mm Greiner CELLSTAR® dish, and 5 mL of 1X-PBS was added. 250 mL of 10X-PBS was made by dissolving 20 g of NaCL (VWR), 0.5 g of KCl (Sigma-Aldrich), 6.8 g of $Na_2HPO_4*7H_2O$ (VWR), and 0.6 g of KH_2PO_4 (VWR) in 100 mL of distilled and deionized (DI) water. The pH was adjusted to 7.4 using a S220 SevenCompact™ pH meter. The volume was filled to 250 mL, and it was run through a sterile filter using a bottle top filtration funnel (VWR). The 10X-PBS was then diluted with DI water to 1X-PBS. After the 1X-PBS was aspirated, 5 mL of Trypsin-EDTA (Mediatech, Inc.) was added to the dish (approximately a quarter of the volume of growth media). Cells were then placed into the incubator for 5 minutes. After the 5 minutes, the cells were removed from the incubator, and 5 mL (or an equal amount of Trypsin-EDTA volume) was added to the cell culture dish. The cells were observed to be detached under a Nikon® Eclipse TE300 microscope. Once this step occurred, the options varied. Depending on the experiment, a fraction of the cells could be added to another 145 mm x 20 mm Greiner CELLSTAR® dish with 20 mL of α-MEM. This would be one cell Passage. However, if the MSCs were to be seeded onto a scaffold, then they would have to be counted. The cells were counted with a Fisher Scientific® Hemacytometer. The cell suspension of Trypsin- α-MEM was centrifuged at 300g on a Thermo Scientific Heraeus Multifuge X1. The cell pellet was then resuspended in an appropriate amount of media for seeding. When seeding the MSCs on the T-Glase scaffolds with PMMA nanofibers, the cell suspension was dropped slowly onto the T-Glase scaffold with PMMA nanofibers. After waiting an hour, the remaining amount of media (usually 1 mL) was added to make 4 mL of media in the 6-well plate.

To freeze cells, instead of resuspending the pellet in normal α-MEM growth media, the MSCs were resuspended in 9 mL of 48% FBS, 52% α-MEM with 10% FBS and 1% Pen/strep. 9 mL of 20% DMSO from Sigma-Aldrich® with 80% α-MEM, 10% FBS and 1% Pen/strep were also added to this cell-media mixture in a slow, drop-wise fashion. The cell suspension was aliquoted into 18 cryo-vials, and placed in a special tray, and submerged in isopropyl alcohol. This special tray was stored at -80 °C for 24 hours. After 24 hours, the cryo-vials were moved into the LS-750 Taylow-Wharton Lab Systems liquid nitrogen tank for long-term storage.

Scaffold/Coverslip Seeding

All the cell seeding took place in CELLSTAR® Cell Culture 6-Well Plates. For the control wells with MSCs placed on the cell culture dish surface, 2 mL of α-MEM was added. For the wells with glass coverslips on the bottom of the cell culture dish, 2 mL of α-MEM was also added. For the wells with scaffolds added, 4 mL of α-MEM was added to ensure that cells near the top portion of the scaffold also receive appropriate nutrients.

For the control wells during the coverslip experiments, as well as the coverslip wells, approximately 150,000 to 180,000 cells were added to each well of the 6-well plate. During the experiments for the T-Glase scaffolds, the control wells were seeded with 80,000 to 120,000 cells. During the same experiments, approximately 500,000 cells were added to the T-Glase scaffolds. This amount of cells was used to ensure that a fraction of the cells would attach to the PMMA nanofiber scaffold.

Scaffold Grid and Coverslip Grids

The scaffold grids made of T-Glase shown in **Figure 6 (A)** were printed with a Rostock Max™ V2 Desktop 3D Printer. Coverslip grids made of T-Glase shown in **Figure 6 (B)** were also printed with a Rostock Max™ V2 Desktop 3D Printer.

pHEMA Hydrogel Coverslip Preparation

Spincoating is a technique used to create a thin layer of polymer on the glass surface of a coverslip. The spincoating was performed using a Laurrell Technologies spin coater (Model Ws-400BZ-6NPP/Lite). Poly(2-hydroxyethyl methacrylate) (pHEMA MW_{avg}= 300,000 Da) was used as the hydrogel on which to prevent MSCs from growing, to ensure that the cells grew on the fibers. A still unresolved component of this experiment is the pHEMA hydrogel layer. A 100 μL of 3% and 1.2% pHEMA in 90:10 ethanol:water that was spin-coated at either 1000 rpm, 2500 rpm, or 3000 rpm,. We placed 150 μL of pHEMA solution onto a 22x22 cm Corning® glass coverslip and heating it at 40 °C for 3 hours. The pHEMA hydrogels were sometimes effective, but many times had tears in them in which the mouse MSCs (MSCs) would grow. The most effective and recently used technique was 3% pHEMA in 90:10 ethanol:water spin-coated on a glass coverslip at 1000 rpm.

Electrospinning

Much of this project was constructed through experimental optimization beginning in September 2013. The first and most critical part of the project was electrospinning adequate

nanofibers on which to place the MSCs. Electrospinning was done in a special electrospinning apparatus shown in **Figure 6 (A)**. The box made of acrylic insulating walls with a high voltage source, a syringe pump from New Era Pump Systems, Inc. Model No. NE-300, and a large copper target. The polymer solution was loaded into a 1 mL syringe from Hamilton Gastight with a 13.8 mm diameter and an 18 GA needle from Weller. Both the coverslip and the T-Glase scaffolds were be taped to the large copper target. The taped scaffold grid is shown in **Figure 6 (A)**.

For the pHEMA-coated coverslips, a solution of 25% m/v PMMA in 1:1 DMF/ tetrahydrofuran (THF) at a distance of 15 cm, with a flow rate of 7 mL/hour, with a voltage of 10 kV, for 1 minute, and a humidity of upwards of 20% was used. A higher humidity produced better fibers with less beading. These nanofibers had a diameter of approximately 1.74 μm. Eventually, these fibers were determined to be too large to adequately mimic the extracellular matrix. The DMF/THF was also found to have autoflourescent properties, which interfered with our immunofluorescence analysis. Then, a combination of 25% m/v PMMA in 90:10 nitromethane:DMF at a distance of 12 cm, with a flow rate of 3 mL/hour, with a voltage of 10-12 kV, and a humidity of upwards of 20% was used.. Although there was more beading in this combination of parameters, the fiber diameter was acceptable.

For the T-Glase scaffold grids, a combination of 30% m/v PMMA in nitromethane at a distance of 12 cm, with a flow rate of 3 mL/hour, with a voltage of 10-12 kV, and a humidity of upwards of 20% was used. This produced acceptable nanofibers without beading.

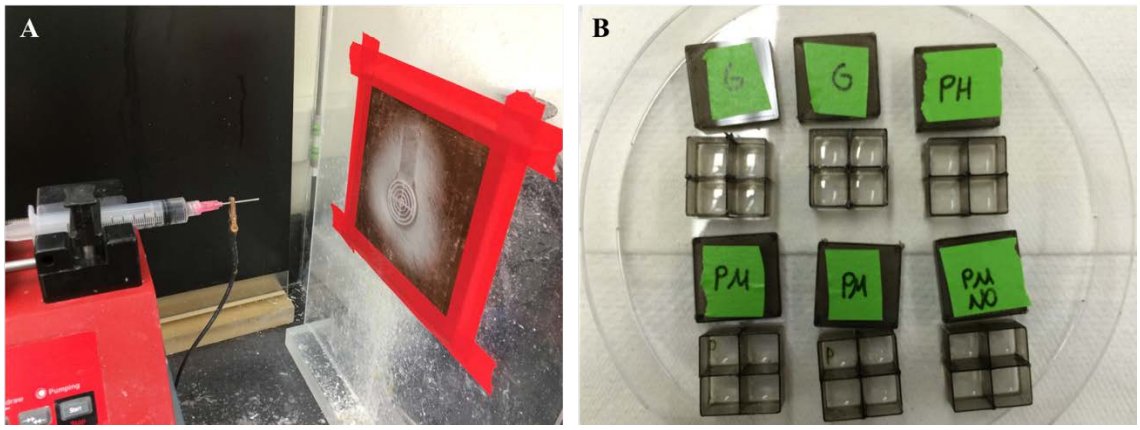

Figure 6: The left photo (A) shows the electrospinning apparatus with the scaffold grid taped to the back of the copper plate. The polymer solution is ejected from the syringe onto the bullseye of the ccaffold grid. The right photo (B) shows T-glase grids glued onto coverslips. "G" stands for glass coverslips, "PH" stands for glass coverslips with pHEMA, "PM" stands for glass coverslips with pHEMA and PMMA nanofibers, and "PM NO" stands for glass coverslips with pHEMA and PMMA nanofibers but no cells.

Nanofiber Diameter Estimation

To determine the average size of the PMMA Nanofibers used on the T-Glase scaffold grids, a T-Glase scaffold grid was imaged in a water immersion objective with a Leica DM5500 B. The size of the nanofibers was determined using ImageJ from the photographs taken using the Leica DM5500 B. The images are shown in **Appendix B**.

Immunofluorescence

Immunofluorescence was used to visualize the differences in the total H3 acetylation, acetylation of H3 K9/K14, and dimethylation of H3 K9. First, the MSC samples from were obtained from 22x22 cm Corning® glass coverslips were either just a glass surface, a pHEMA hydrogel, or a pHEMA surface with PMMA nanofibers spun over the hydrogel. These glass coverslips were carefully removed from each well, and placed in a new 6-well plate. Each coverslip was then washed with 1X-PBS to remove any excel cell culture media. Then,

Cytoskeletal Stabilization Buffer (CSB) was added for 1 minute to fix the cytoskeleton. Cytoskeletal Stabilization Buffer is made by adding 50 mM of NaCl, 0.5% Triton X100, 10 mM PIPES, 2.5 mM $MgCl_2$, 1 mM EGTA, 0.3 M Sucrose, and protease inhibitors and phosphate inhibitors both at a dilution of 1:100. After 1 minute, the CSB was aspirated, and 1 mL of the Fixation Buffer (FB) was added for 15 minutes to immobilize the antigens. FB is made with 3.7% - 4% Paraformaldehyde in 1X PBS. Then, the Permeabilization Buffer (PB) was added to allow access of the antibody to the antigen, and the coverslips were incubated for 45 minutes. PB is made with 1X PBS, 3% BSA, and 0.1% Triton X-100. Then, the PB was aspirated, and primary antibodies for either dimethylated H3 K9, total acetylated H3, and total H3 were added at 1:400 in PB and incubated for one hour. Then, the primary antibody solution was aspirated, and the coverslips were washed 3 times with 1X-PBS. The secondary antibodies for the 800 nm and 680 nm channels, respectively, were added with PB and incubated for 45 minutes in the dark. Once again, the solution was aspirated and the coverslips were washed 3 times with 1X-PBS. Phalloidin from Biotium was added at a 1:1000 dilution and incubated for 30 minutes in the dark, followed by aspiration, and washing 3 times with 1X-PBS. DAPI from VWR was added at a 1:5000 dilution, and incubated for 15 minutes. The coverslips were mounted to VWR microscope slides with 30 μL of Prolong Gold antifade reagent from Life Technologies. These coverslips were sealed with nail polish. The coverslips were imaged and analyzed under a Leica® DM5500B.

In-Cell Western

A technique that was used for the coverslips with the grids shown in **Figure 1** to quantify epigenetic expression was the In-Cell Western. The same protocol for Immunoflourescence was used, just instead of 1 mL of reagents being used over the entire, only 200 µL was used in each individual grid well.

Cell Lysis for 24 Hour Experiment

The RIPA lysis buffer was initially used to lyse the cells, but as explained in the results and shown in **Appendix A**, it did not allow for the expression of histone proteins in any samples. Therefore, it was replaced by the M-PER lysis buffer. The Halt™ Protease Inhibitor Cocktail (100X) was added at 1:100 to the M-PER lysis buffer. For the control 6-well plates, 200 µL of the M-PER lysis buffer with the protease inhibitor was added, while 400 µL was added to the plates with the T-Glase scaffold grids. The RIPA and M-PER lysis buffers were used to lyse the samples at 4 °C, each at a concentration of 1mL per 10^6 cells. The 400 µL for the T-Glase scaffold grids was added to ensure that the surfaces of all the fibers could be accessed by the lysis buffer so as to collect the maximum amount of cell lysate.

Before adding the lysis buffer, the media was aspirated, and both the control and T-Glase scaffold grid wells were washed with 1X-PBS three times to ensure that the media has been completely removed from the wells. The samples were vortexed or shaken to remove the lysis samples from the scaffolds. Then, the samples were pipetted into vials and frozen at -80 °C. Samples were then thawed only once to minimize protein degradation.

Cell Lysis for Heritable Study

The purpose of this method is examine whether the epigenetic and other protein changes that occurred due to the PMMA nanofibers fibers would be preserved, even when the MSCs were taken off the PMMA nanofibers. 24 hours after the cells had been seeded, 2 mL of 1X-PBS was added to each well of the 6-well plate. The 1X-PBS was then aspirated off. Then, 1 mL of Trypsin-EDTA was added, and the 6-well plate was put into the incubator for 5 minutes. Once all the cells have detached, 1 mL of α-MEM was added to the cell suspension. Then, the cells were then reseeded in a new 6-well plate and left to grow for another 24 hours. The next day, 200 µL of the M-PER lysis buffer with the protease inhibitor was added to the wells with cells from the control as well as those from the T-Glase scaffold grids with PMMA nanofibers. Following the addition of the lysis buffer, the samples were vortexed or shaken to remove the lysis samples from the scaffolds. Then, the samples were pipetted into vials and frozen at -80 °C. Samples were then thawed only once to minimize protein degradation.

Western Blot

Before beginning the western blot, the running and transfer buffers were made. To make running buffer, combine 500mL of DI water with 8.7g of Tris-Glycine Buffer and 10mL of 10% SDS solution. To make 1500 mL of the transfer buffer, combine 1250 mL of DI water with 26.1 g of Tris-Glycine Buffer, then fill to 1500 mL. To make 10X-TBST-Tween, combine dI water with 50 mM Tris, 150 mM NaCl, 0.05% Tween 20, and adjust the pH to 7.6.

Then, the gel must be run. First, a 10% gel must be cast to ensure that the 17 kDa proteins such as Acetylated H3K9/14 and dimethylated H3 K9/K14K9 are detected. The 10%

SDS acrylamide gel was cast using DI water, 40% Acryl-bisacrylamide, 1.5 M Tris at 8.8 pH, 10% SDS, 10% Ammonium persulfate, and TEMED. The gel was cast in a Hoefer dual caster. Two molecular protein ladders are loaded on the two end lanes of the gel. Then, a 90:10 solution and 4X protein loading buffer (LI-COR) of β-mercaptoethanol was added to the proteins samples, and the protein samples were then heated at 95 °C. This denatured the proteins, so as to visualize them on the gel. Then, the protein samples loaded into the gel after normalizing for total protein concentration, and the gel was run at 120 V for 3-4 hours.

Once the gel is finished running, prepare to complete the transfer step. The gel is removed from the glass plates, and a polyvinylidene difluoride (PVDF) membrane is laid on top of it, following PVDF membrane activation in methanol for 5 minutes. The membrane and the gel are placed in between four pieces of filter paper with two on each side. This stack is then placed in between 2 reusable black foam pads and submerged in the transfer apparatus with the transfer buffer. Transfer occurred at 80 V for 80 minutes.

Following the transfer step, the PVDF membrane is removed from the transfer apparatus, and a 5% bovine serum albumin (BSA)/ Tris-buffered saline with Tween 20 (TBST) is added to block overnight at 4 °C. Following this blocking step, the membrane was incubated with primary antibodies in 5% BSA-TBST solution either overnight at 4 °C, or for one hour at room temperature. Every membrane was stained with α-tubulin (B-1-2-5) to be a control between groups to normalize for the amount of cells. Other primary antibodies that were used were acetylated H3 (AH3-120), acetylated H3 (Lys 9/14), and total H3. All four of these were from Santa Cruz Biotechnology, Inc. The phospho-p44/42 MAPK (Erk1/2) T202/Y204 primary antibody is from Cell Signaling Technology, Inc. The other antibodies that were used were the

dimethylated H3 (K9) and the dimethylated H3 (K4) antibodies, both from Abcam, Inc. Every antibody that was used had a dilution range of 1:1000.

Following primary antibody incubation, the membrane is washed 3 times with TBST, and then the membrane is incubated in the secondary antibody for one hour at room temperature. The secondary antibodies are either IR dye 800GCW IgG (donkey anti-mouse, LI-COR) or IR dye 680 IgG (goat anti-rabbit, LI-COR) at a dilution of 1:5,000. After this secondary step is complete, the membrane is washed 3 times with TBST, and then scanned and analyzed under the LI-COR Odyssey®. The quantification of the Integrated Intensity of the western blot bands was done by the Odyssey® CLx imaging system.

DNA Methylation

Another perspective through which to understand epigenetic changes is through detecting the Methylation of DNA. The first step is to isolate the DNA using the DNA Concentrator Kit from Epigenentek. The components of the reagents were not disclosed by Epigentek. After the cells were lysed using the RIPA lysis buffer at concentration of 1 mL per 10^6 cells, three freeze-thaw cycles were performed to break up the nucleus of the MSCs. The cell lysis samples were then added to a centrifuge column with 2 volumes of reagent. Then, the column was centrifuged at 12,000 rpm for 15 seconds. The flowthrough was discarded, and another 200 μL of reagent was added, and the column was centrifuged again at 12,000 rpm for 15 seconds. The same 200 μL of reagent was added, and the column was centrifuged again at 12,000 rpm for 30 seconds. Finally, the column was placed in a new 1.5 mL vial, and 8 μL of Final DNA Elution Buffer was added. The column was then centrifuged at 12,000 rpm for 30

seconds. The flow-through with concentrated DNA was analyzed on a Thermo Scientific™ NanoDrop 2000.

Once the DNA concentrations of the lysis samples were determined, the Methylamp™ Global DNA Methylation Quantification Ultra Kit was used to detect DNA Methylation. The components of the reagents were not disclosed by Epigentek First, approximately 28 μL of sample reagent was added to each of the sample wells, followed by 2 μL of a constant amount of DNA samples between 100-200 ng. A standard curve for positive DNA was added in the remaining wells with approximately 28 μL of sample reagent followed by 2 μL of the positive control DNA at varying concentrations. A negative control well was made too, with 28 μL of sample reagent followed by 2 μL of Negative Control DNA. The wells were incubated at 37°C with no humidity for 40 min, followed by incubation at 60°C with no incubation for 35 to 40 min to evaporate the solution and dry the wells. Once the wells have completed dried, another reagent was added to each sample well, and the wells were again, incubated at 37°C with no humidity for 30 min. This reagent was aspirated, and another washing reagent was used to wash each sample well three times. Then, a primary antibody was added at a dilution range of 1:1000 range to the washing reagent at a concentration of 1 μg/ml. 50 μL of another reagent was added, and each well was incubated for 60 minutes. Once this step was complete, the wells were aspirated and washed four times with the washing reagent. A secondary antibody was added at a 1:10,000 to 1:50,000 ratio into the washing reagent. Once again, the wells were aspirated and washed five times with the washing reagent. 100 μL of another reagent was added to each well, and the wells were incubated at room temperature for 1-5 minutes away from the light. After the color for the “middle” of the standard curve turns medium blue, add 50

μL of a final reagent to stop the reaction. Then, the completed assay was analyzed on a microplate reader.

Chapter 3
Results

Initial Western Blot Attempts

For the first year of the project, western blot analysis was used to determine the amount of the methylation and acetylation of the histone proteins. There was much difficulty involved with this method, due to failure to collect enough protein from the lysates collected from the MMA nanofibers. The MSCs were placed on the pHEMA-coated PMMA nanofiber coverslips, the cells were lysed, and the cell lysis was run on the western blot. This method using coverslips was abandoned after several months, and the in-cell western blot analysis was used. For all the western blots done during this portion of the project, the RIPA lysis buffer was used. However, the RIPA buffer clearly did not facilitate the detection of the dimethylated H3 K9 protein, as shown in **Table 1**.

In-Cell Western Blot Analysis

After it was determined that there was not enough protein and cell lysate available to detect the epigenetic changes, the in-cell western blot was attempted. This technique is more similar to immunofluorescence, but the protein expression is quantifiable on the LI-COR. The results showed that there was an epigenetic response caused by the PMMA nanofibers on the MSCs. **Figures 7 and 8** are examples of the visualization of the in-cell western blot analysis on the LI-COR at the 800 (green) channel with dimethylated H3 K9, and the 700 (red) channel with total H3. Each coverslip was divided into individual quadrants or wells separated by the T-Glase grids, which allowed them to be treated as independent samples to increase the statistical significance. The absorption values for each quadrant of each slide slide was measured, and the results for these particular slides are shown in Figure 6.

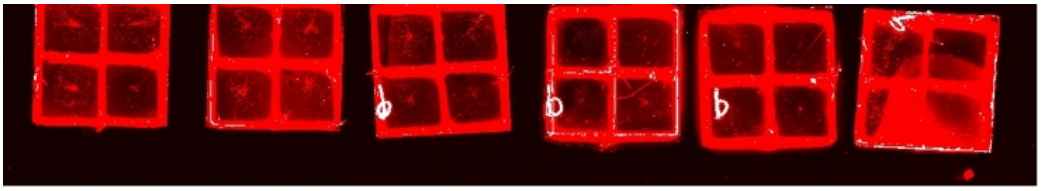

Figure 7: This figure shows the in-cell western blot for the 800 channel with dimethylated H3 K9/K14K9. From right to left, the first two coverslips are the class control slides, the middle two coverslips are the pHEMA-coated PMMA nanofiber coverslips, and the right two covserlips are the pHEMA control coverslips.

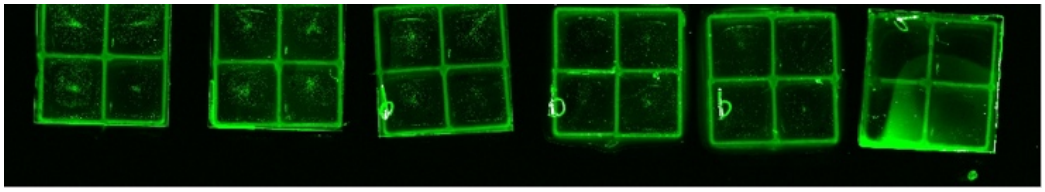

Figure 8: The figure shows the in-cell western blot for the 700 channel with TOTAL H3. From right to left, the first two coverslips are the class control slides, the middle two coverslips are the pHEMA-coated PMMA nanofiber coverslips, and the right two coverslips are the pHEMA control coverslips.

The results of the preliminary in-cell western, shown in **Figure 9**, display a decrease after 24 hours in the dimethylated H3 K9 and total acetylated H3. The relative expression values were found as the ratio of total acetylated H3 to the total H3 total and dimethylated H3 K9 to total H3. Total H3 acted as the control, since it represents the overall number of histone proteins expressed in the MSCs.

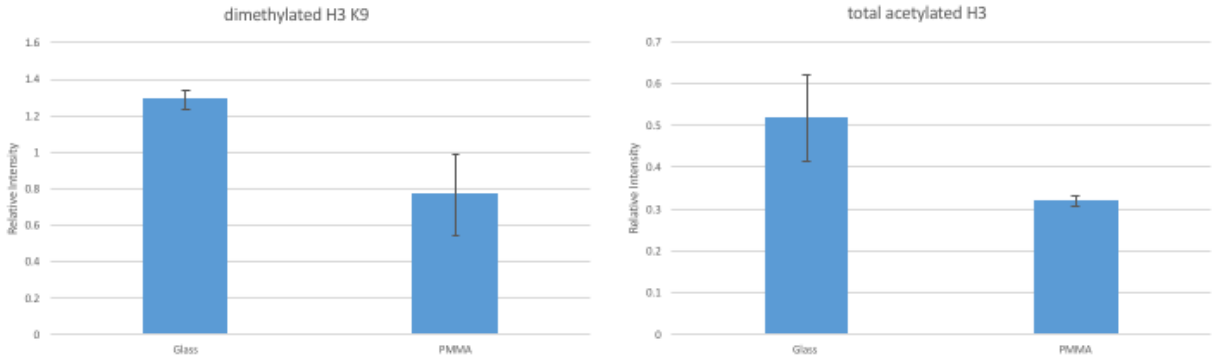

Figure 9: Normalized protein expression to total H3 of dimethylated H3 K9 and total acetylated H3. MSCs were seeded on Glass coverslips (N = 2) or pHEMA-coated coverslips with PMMA nanofibers (N = 2).

However, these preliminary results were not completely replicated, as shown in **Figure 10**. More data points were included than in **Figure 9**. **Figure 10** does not show a statistically significant decrease in acetylated H3, but Figure 10 shows a statistically significant decrease in

dimethylated H3 K9. Another point of concern with our data from **Figures 7 and 8**, which are graphically represented in **Figure 10**, is the failure of the pHEMA control slide. The pHEMA control slide did not result in cell apoptosis. The in-cell western confirmed that the MSCs on the glass pHEMA-coated coverslips displayed protein expression levels comparable to that of the glass coverslips. This completely eliminates the point of having the pHEMA coverslip as the negative control.

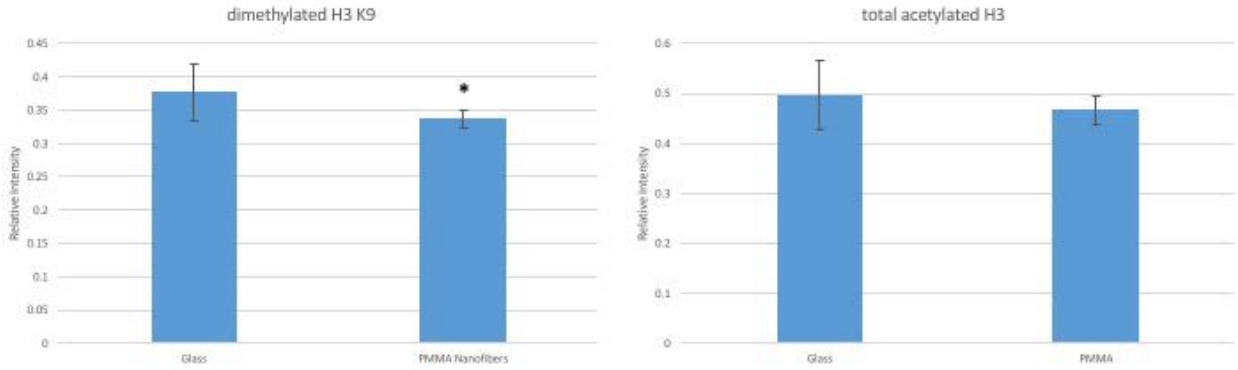

Figure 10: Normalized protein expression to total H3 of dimethylated H3 K9 and total acetylated H3. MSCs were seeded on Glass coverslips (N = 6) or pHEMA-coated coverslips with PMMA nanofibers (N = 6).

Immunofluorescence

The results from immunoflourescence are shown in **Figure 11**. It is hard to visually discern whether there was a change in protein expression levels from the glass coverslips to the glass coverslips with pHEMA and PMMA fibers, but it does show that MSCs were living on the PMMA Nanofibers.

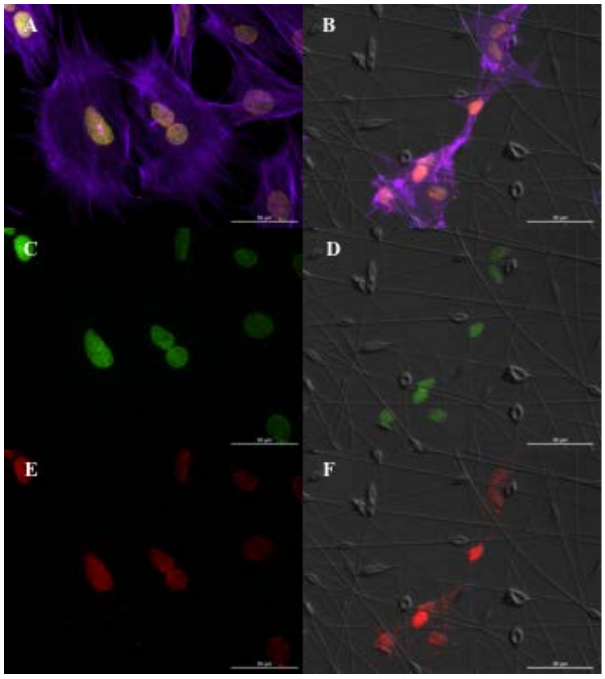

Figure 11: Purple is Actin, green is dimethylated H3 K9/K14, and red is acetylated H3. (A) and (B) are the overlay of all three proteins, (B) and (C) are of the dimethylated H3 K9/K14 antibody, while (D) and (E) are of the acetylated H3 antibody.

DNA Methylation

Figure 12 shows that there is a statistically insignificant decrease in DNA Methylation from the MSCs on a glass control surface vs. the PMMA nanofiber scaffold. Although this is a

potentially promising avenue, isolating DNA from the cell lysis samples proved much more difficult than anticipated. Therefore, this was the only measurement of DNA Methylation

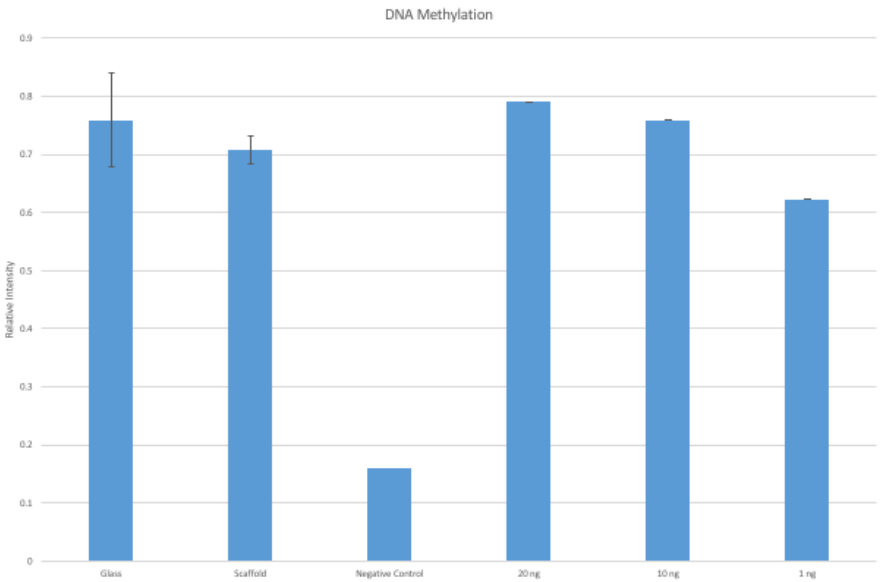

Figure 12: Glass (N = 2) and Scaffold (N = 2) represent the two conditions onto which the MSCs were seeded. The results were insignificant (p = 0.27051).

Western Blot

The M-PER cell lysis buffer was shown to be much more effective at isolating at the dimethylated H3 K9 protein than the RIPA cell lysis buffer which had been used in all previous western blot experiments. Therefore, the M-PER cell lysis buffer was used for all of the proteins that were analyzed in this study. This is demonstrated in **Table 1**.

Table 1: Comparison of M-PER to RIPA with dimethylated H3 K9 using western blot bands.

M-PER (N = 3)	RIPA (N = 3)

α-tubulin	
dimethylated H3 K9	

24 Hours on PMMA Nanofibers

Table 2 displays the western blot bands, while **Figure 13** shows the quantitative analysis of the relative intensities. **Figure 13** shows increase in dimethylated H3 K9, which is a discrepancy from the protein expression levels shown in **Figures 14 and 15**.

Table 2: Western blot results of dimethylated H3 K9.

	Control (N = 3)	PMMA Nanofibers (N = 3)
α-tubulin	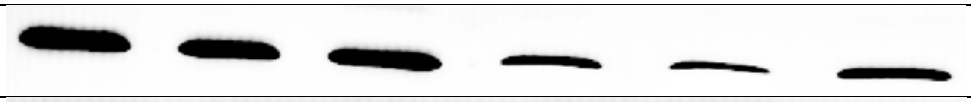	
dimethylated H3 K9		

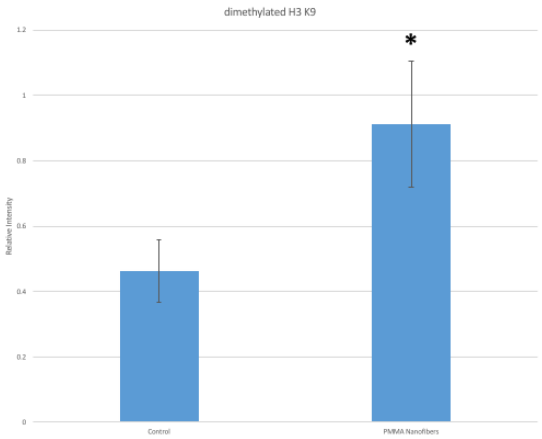

Figure 13: The Control (N = 3) and PMMA Nanofibers (N = 3) represent the two conditions onto which the MSCs were seeded. ("*" = $p < 0.05$)

Table 3 displays the western blot bands, while **Figure 14** shows the quantitative analysis of the relative intensities of dimethylated H3 K9, Erk1/2, and dimethylated H3 K4. All of the protein expression levels were normalized to α-tubulin. All of the normalized protein levels decreased when placed on the PMMA nanofiber scaffolds. However, the decreases in dimethylated H3 K9 and dimethylated H3 K4, as explained in Huang et al., show that the PMMA nanofibers are increasing the likelihood of osteogenesis.

Table 3: Western blot results of dimethylated H3 K9, Erk1/2, and dimethylated H3 K4

	Control (N = 3)	Scaffold (N = 3)
α-tubulin	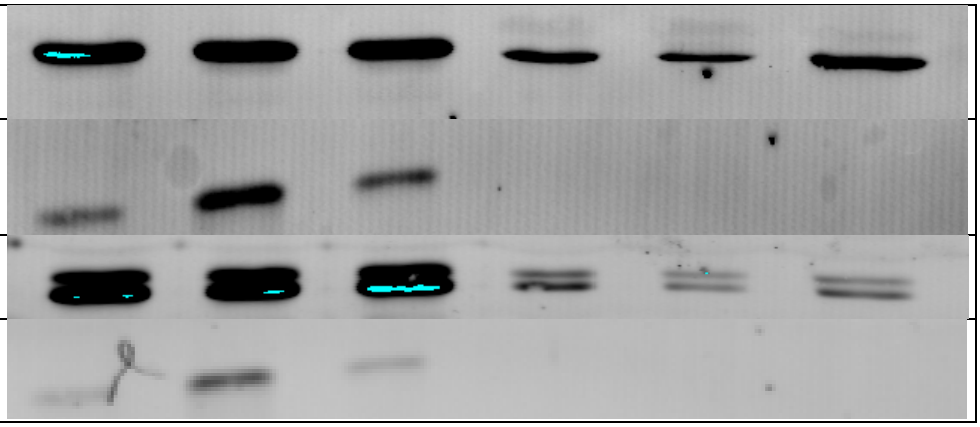	
dimethylated H3 K9		
Erk1/2		
dimethylated H3 K4		

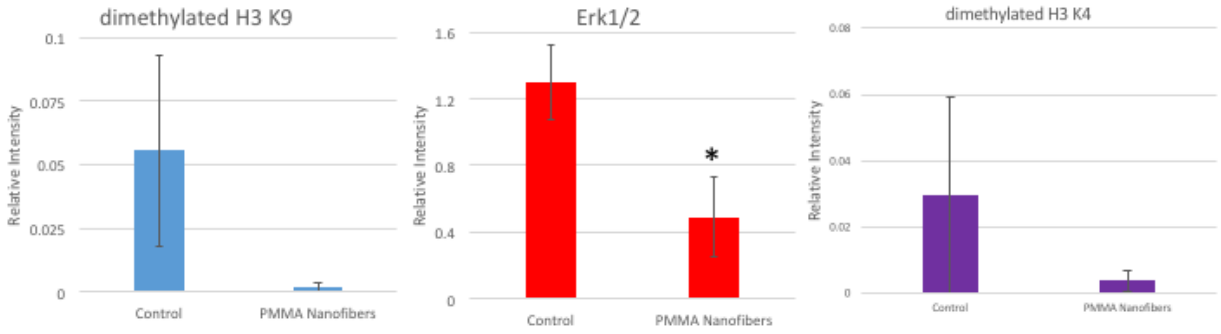

Figure 14: Normalized protein expression to α-tubulin of dimethylated H3 K9, Erk1/2, and dimethylated H3 K4. The Control (N = 3) and PMMA Nanofibers (N = 3) represent the two conditions onto which the MSCs were seeded. ("*" = $p < 0.05$)

Table 4 displays the western blot bands, **Figure 15** shows the western blot expression of dimethylated H3 K9, and acetylated H3 K9/K14 all normalized to α-tubulin. Total acetylated H3 is normalized to total H3. There was a decrease in protein expression for all of these proteins. This is another confirmation that the PMMA nanofibers are encouraging osteogenesis.

Table 4: The changes in dimethylated H3 K9, acetylated H3 K9/K14, total acetylated H3, and Erk1/2 following seeding on Control and PMMA Nanofiber surfaces. Dimethylated H3 K9 and acetylated H3 K9/K14 was normalized to α-tubulin, total acetylated H3 was normalized to total H3, and Erk1/2 was also normalized to α-tubulin.

	Control (N = 3)	Scaffold (N = 3)
α-tubulin dimethylated H3 K9 acetylated H3 K9/K14		
α-tubulin total acetylated H3 total H3	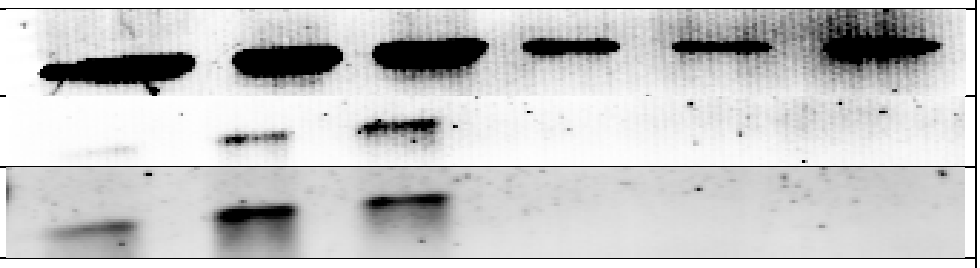	
α-tubulin Erk1/2	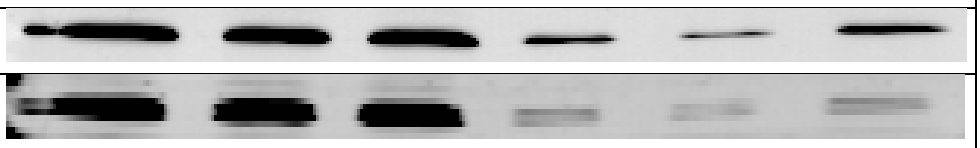	

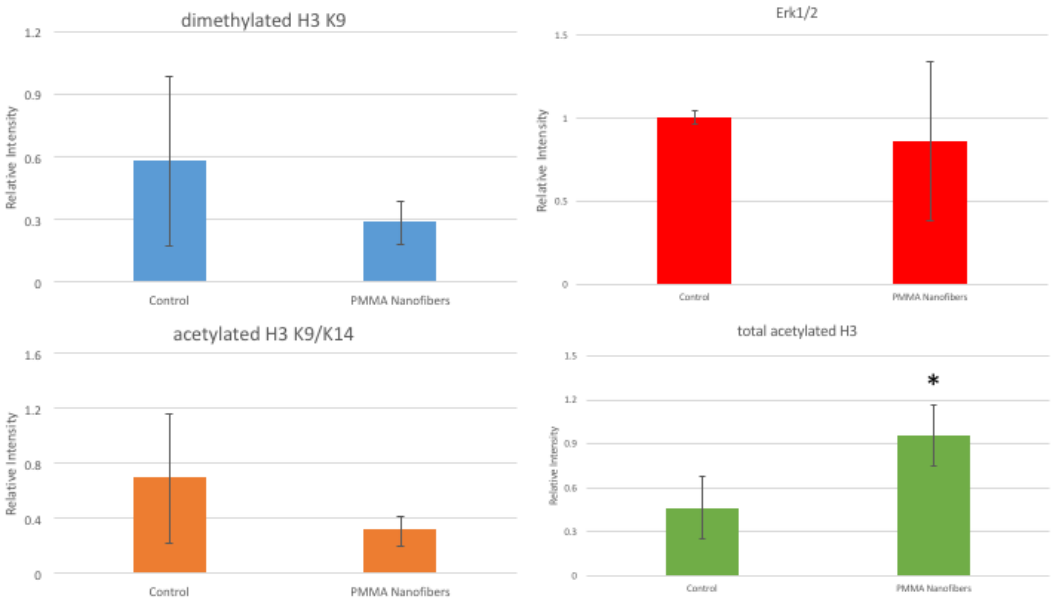

Figure 15: Normalized protein expression to α-tubulin of dimethylated H3 K9, Erk1/2, and acetylated H3 K9/K14. Total acetylated H3 is normalized to total H3. The Control (N = 3) and PMMA Nanofibers (N = 3) represent the two conditions onto which the MSCs were seeded. ("*" = $p < 0.05$)

Are Post-Translational Modifications Heritable?

In **Table 5** and **Figure 16**, the protein analysis from **Table 4** and **Figure 15** was repeated. However, after 24 hours on the PMMA Nanofibers, the MSCs were removed and placed on a flat, control surface for another 24 hours. It is assumed that the MSCs had enough to divide at least once. Therefore, the MSCs that are being analyzed may have their epigenetic markers inherited from the parent cells. **Table 5** displays the western blot bands, **Figure 15** shows the western blot expression of dimethylated H3 K9, and acetylated H3 K9/K14 all normalized to α-tubulin. Total acetylated H3 is normalized to total H3. There was a decrease in protein expression for all of these proteins. Therefore, the post-translational modifications are heritable, as the epigenetic changes were conserved and passed onto their progeny following a 24 hour removal from PMMA nanofibers.

Table 5: The changes in dimethylated H3 K9, acetylated H3 K9/K14, total acetylated H3, and Erk1/2 following seeding on Control and PMMA Nanofiber surfaces and then re-seeding onto a flat surface. Dimethylated H3 K9

and acetylated H3 K9/K14 was normalized to α-tubulin, total acetylated H3 was normalized to total H3, and Erk1/2 was also normalized to α-tubulin.

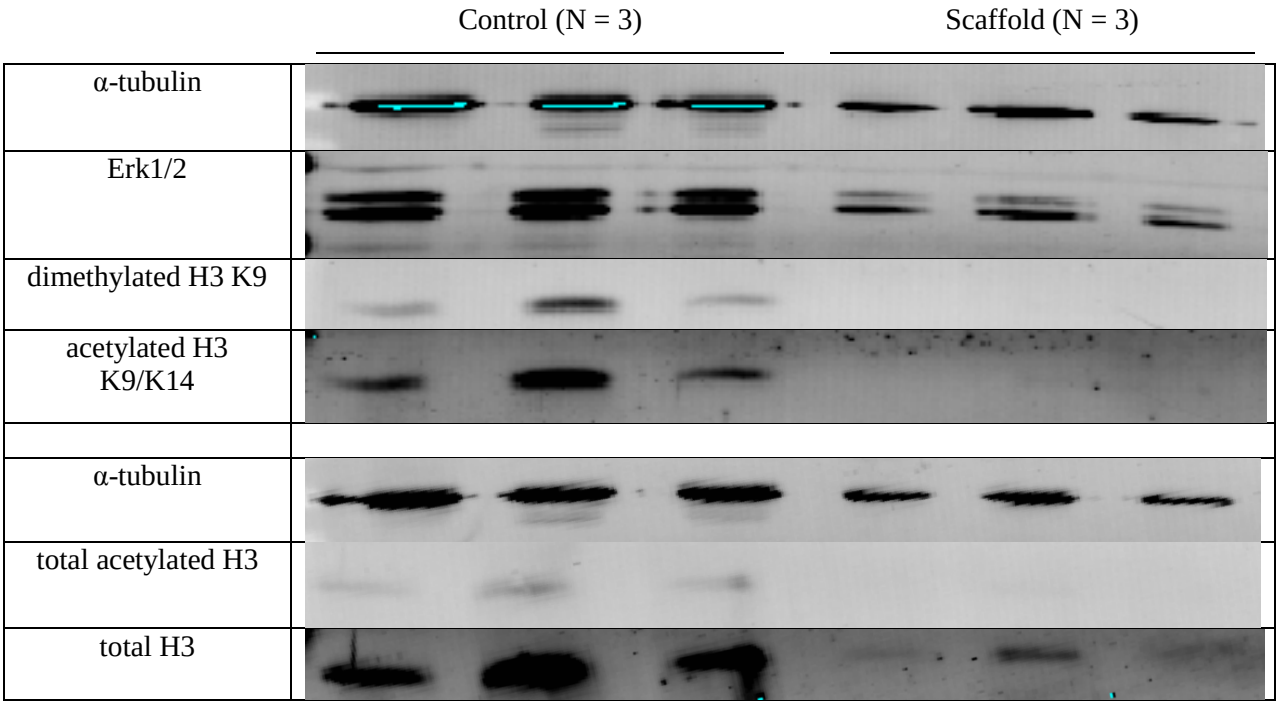

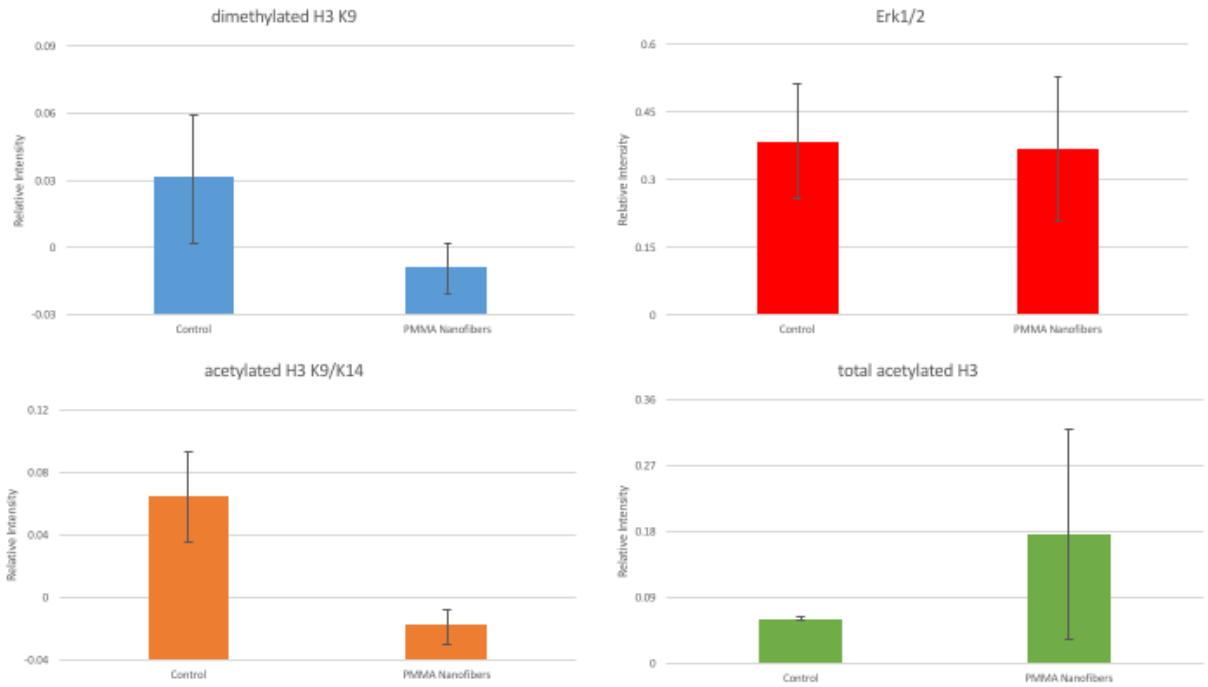

Figure 16: Normalized protein expression to α-tubulin of dimethylated H3 K9, Erk1/2, and acetylated H3 K9/K14. Total acetylated H3 is normalized to total H3. The Control (N = 3) and PMMA Nanofibers (N = 3) represent the two conditions onto which the MSCs were seeded and then re-seeded onto a flat surface.

Table 6 and **Figure 17** are replications of the heritability experiments shown in **Table 5** and **Figure 16**. The expression of Erk1/2 and total acetylated H3 were normalized to total H3. α-tubulin was also included, but no quantitative analysis was performed on using its bands.

Table 6: The changes in dimethylated H3 K9, acetylated H3 K9/K14, total acetylated H3, and Erk1/2 following seeding on Control and PMMA Nanofiber surfaces and then re-seeding onto a flat surface. Dimethylated H3 K9 and acetylated H3 K9/K14 was normalized to α-tubulin, total acetylated H3 was normalized to total H3, and Erk1/2 was also normalized to α-tubulin.

	Control (N = 3)	Scaffold (N = 3)
α-tubulin	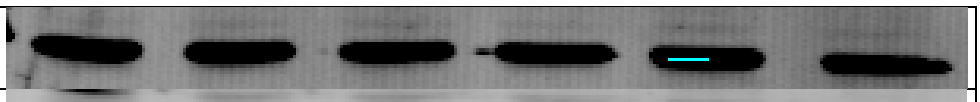	
Erk1/2		
total acetylated H3	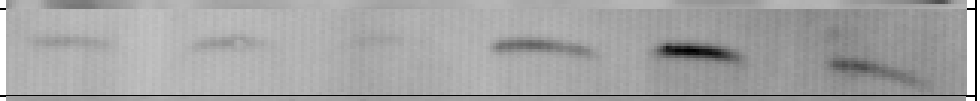	
total H3		

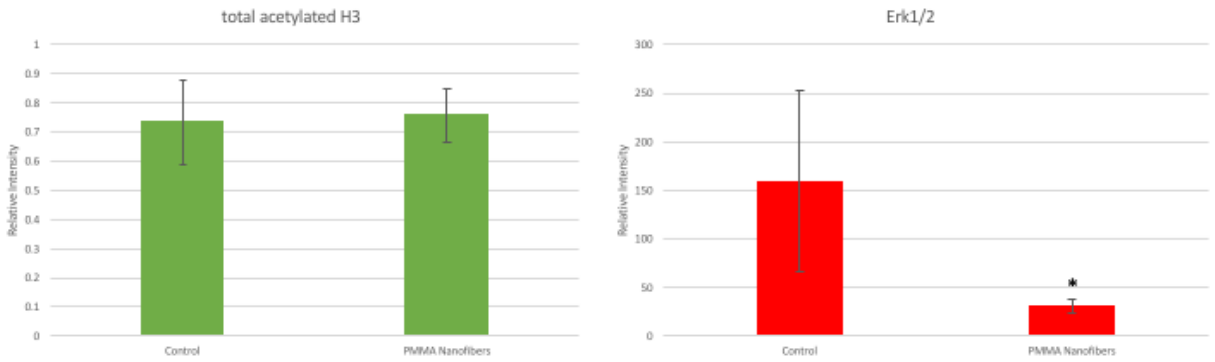

Figure 17: Normalized protein expression to total H3 of total acetylated H3 and Erk1/2. The Control (N = 3) and PMMA Nanofibers (N = 3) represent the two conditions onto which the MSCs were seeded and then re-seeded onto a flat surface.

Table 7 shows a summary for all the western blot data conducted on the various post-translational modifications along with Erk1/2.

Table 7: Summary of Quantitative Western Blot Protein Data

Seeed on PMMA Nanofibers for 24 hrs.	
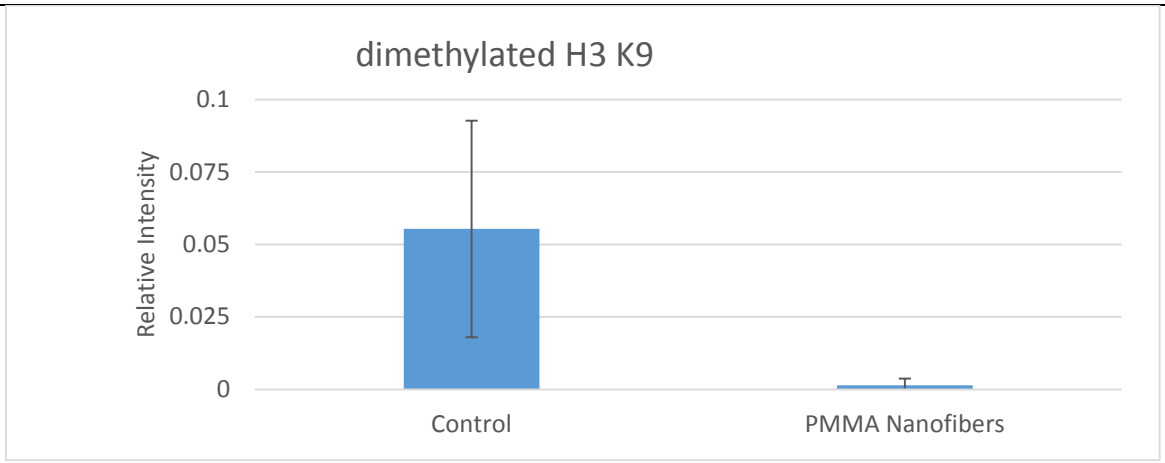	
Normalized to α-tubulin	Normalized to α-tubulin
Seeded on PMMA Nanofibers for 24 hrs., then re-seeded on flat surface for 24 hrs.	

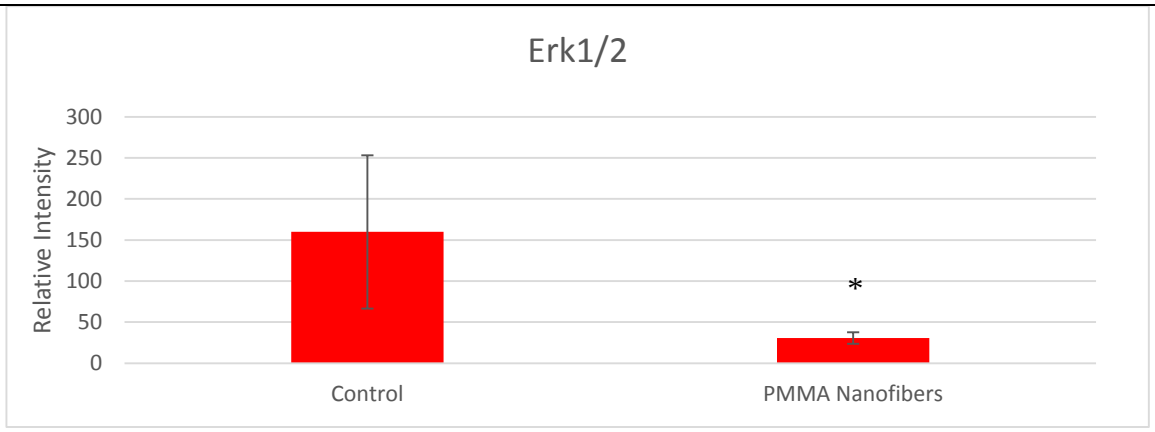

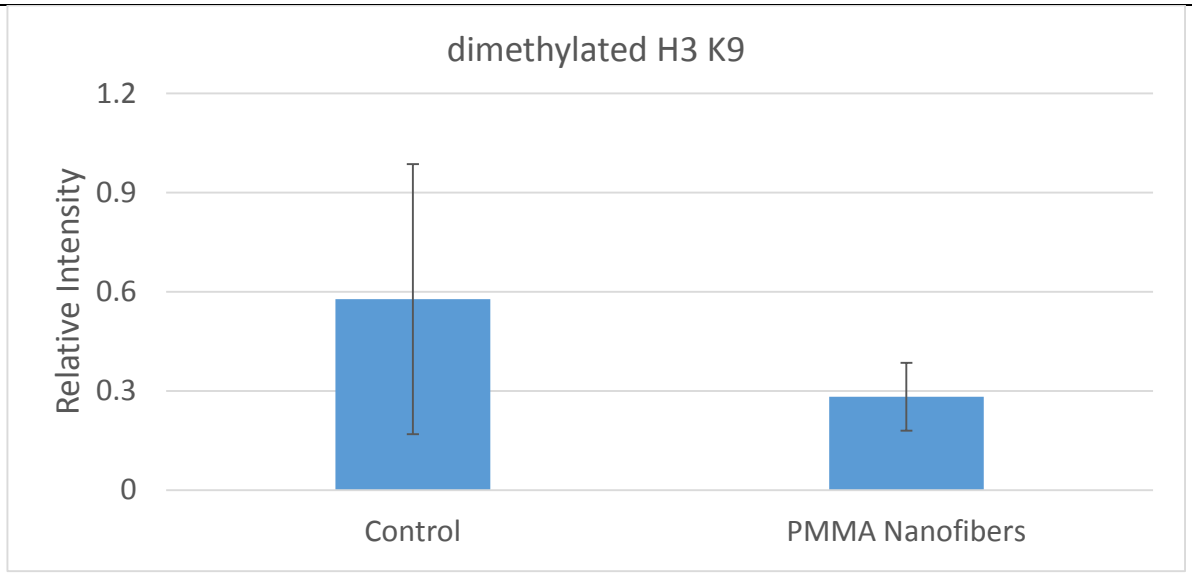

Normalized to α-tubulin

Seeed on PMMA Nanofibers for 24 hrs.

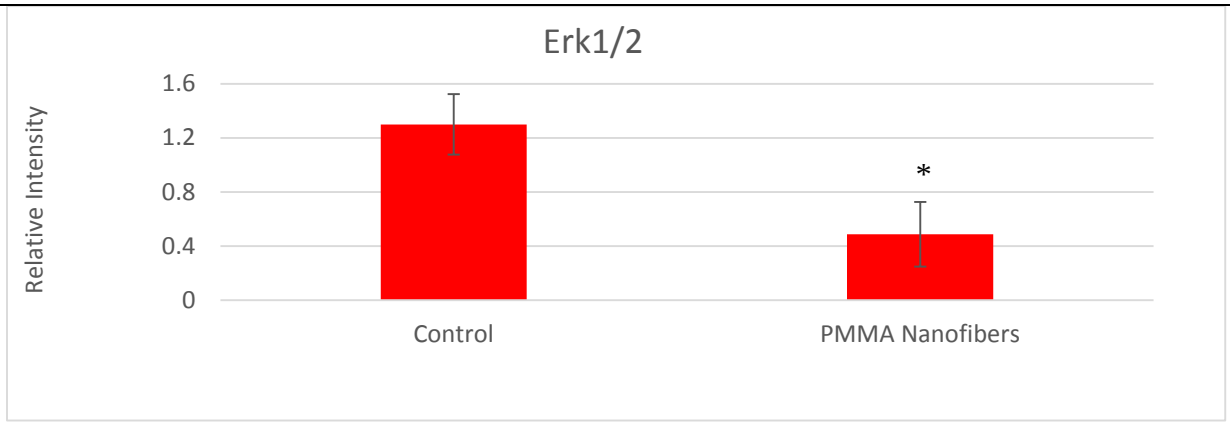

Normalized to α-tubulin	Normalized to α-tubulin
Seeded on PMMA Nanofibers for 24 hrs., then re-seeded on flat surface for 24 hrs.	
Normalized to α-tubulin	Normalized to total H3
Seeed on PMMA Nanofibers for 24 hrs.	**Seeded on PMMA Nanofibers for 24 hrs., then re-seeded on flat surface for 24 hrs.**
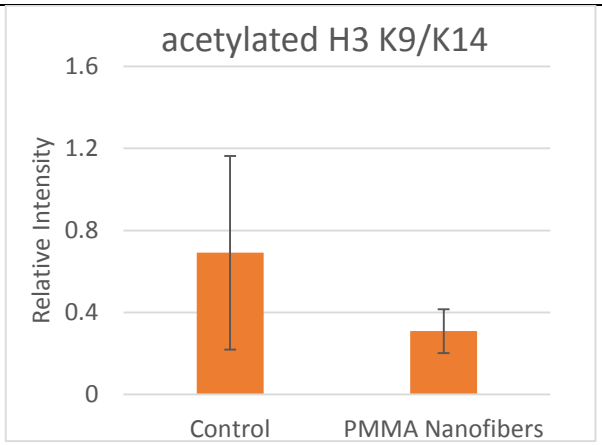	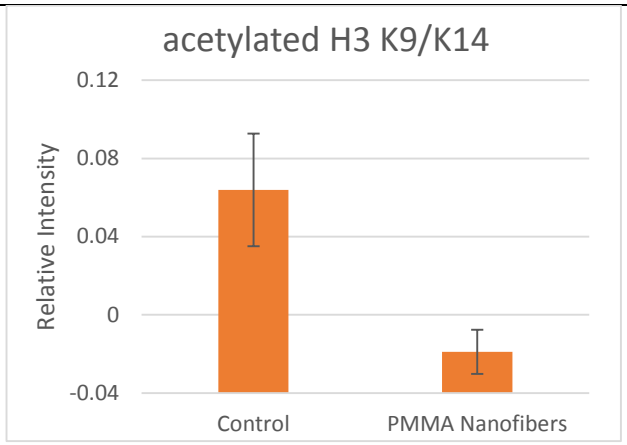
Normalized to α-tubulin	
Seeed on PMMA Nanofibers for 24 hrs.	

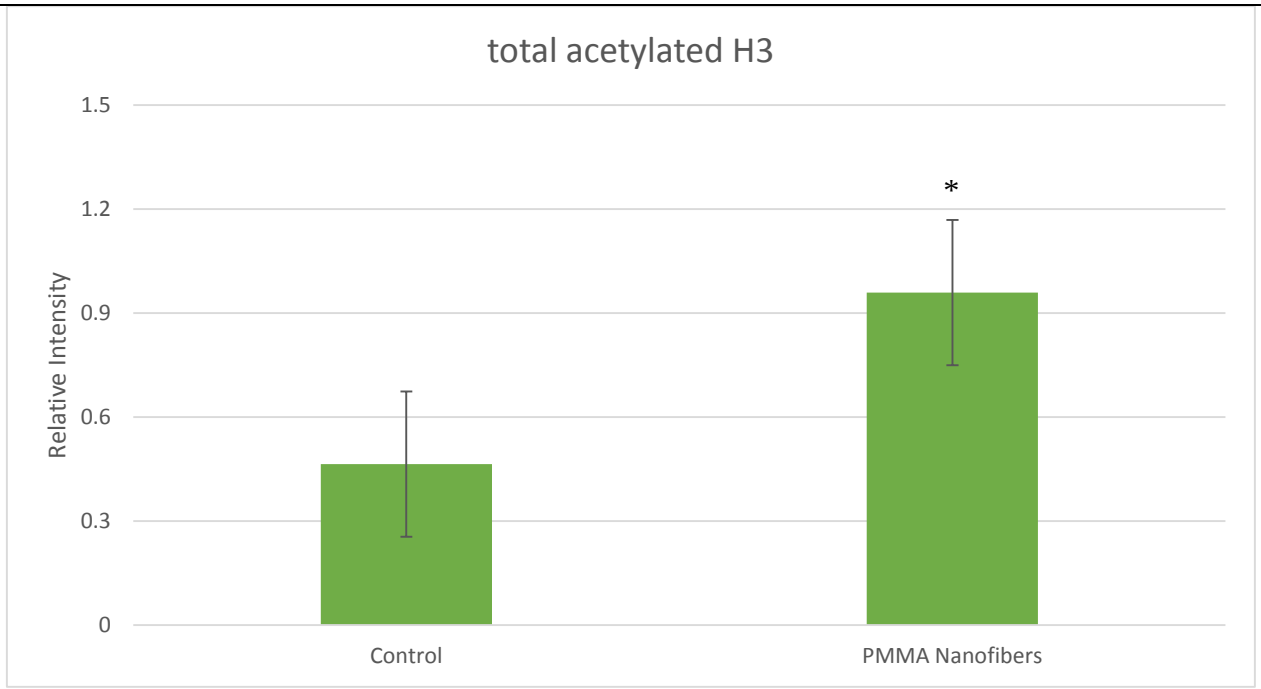

Normalized to total H3

Seeded on PMMA Nanofibers for 24 hrs., then re-seeded on flat surface for 24 hrs.

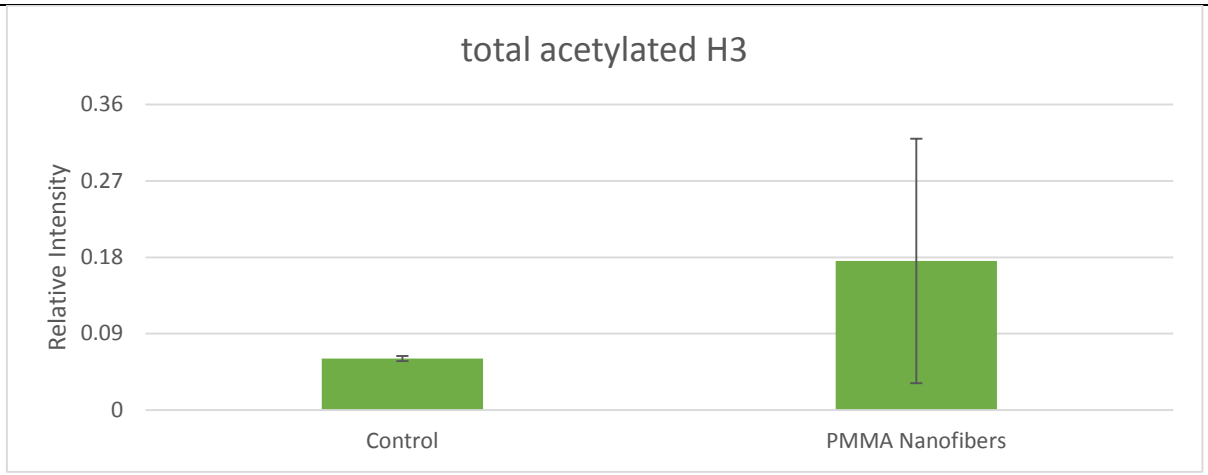

Normalized to total H3	Normalized to total H3

Seeed on PMMA Nanofibers for 24 hrs.

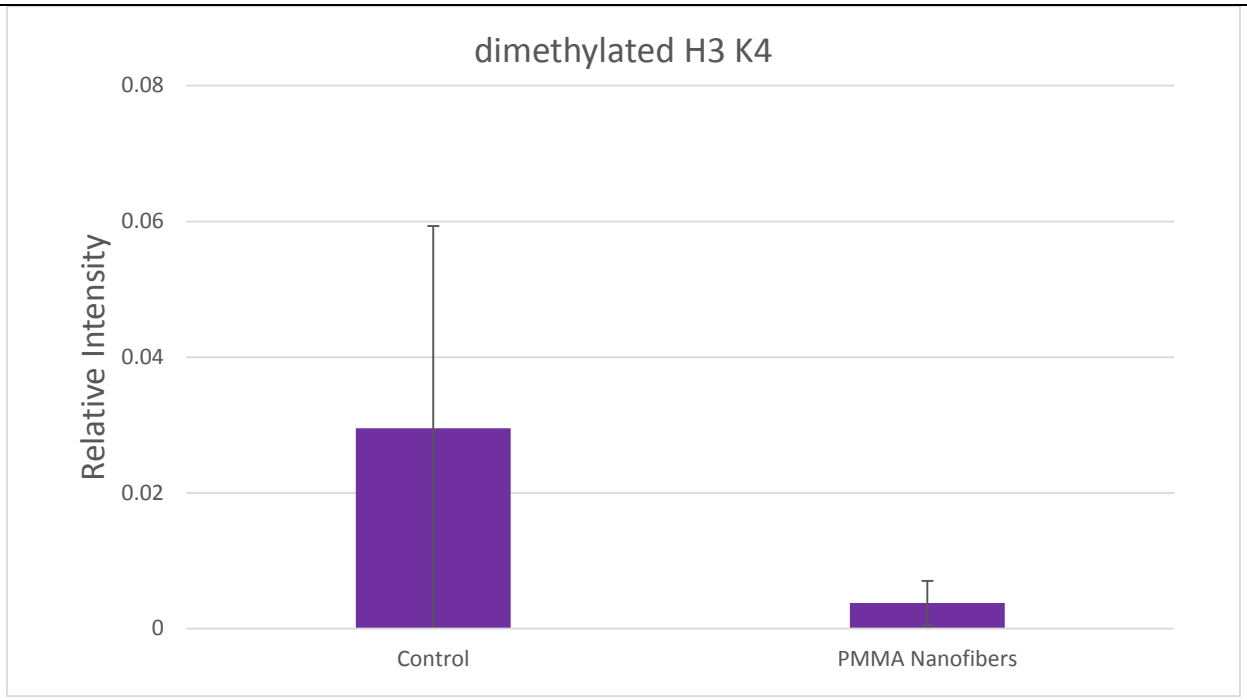

Normalized to α-tubulin

Chapter 4

Conclusions and Future Directions

There was a decrease in most of the proteins shown to regulate the transcription of DNA. This is especially true of that of dimethylated H3 K9, which showed a down regulation in both the in-cell western and the two western blot results. As shown in Ozdemir et al., larger PMMA nanofibers (> 2 μm) reprogram cells toward osteogenesis. This is in contrast to a previous study, where nanogrooves (not nanofibers), were shown to direct the cells toward a more pluripotent state and facilitate induced pluripotency (Downing et al., 2013b). Most importantly, Downing et al. showed an upregulation of dimethylated H3 K4, total acetylated H3, and total H3. If increased osteogenesis and increased pluripotency can be thought of as "opposite directions", the results of this study would show that the MSCs are moving away from a more pluripotent state to more restricted lineage, like that of a somatic cell. However, there was found increase in total acetylated H3, which is consistent with that of Downing et al., unlike the dimethylated H3 K9, acetylated H3 K9/K14, and dimethylated H3 K4.

Another important result was that the epigenetic marker decreases were found to be consistent following re-seeding onto a flat surface for another 24 hours, following the seeding onto PMMA Nanofibers for 24 hours. For example, there was a consistent decrease in Erk1/2, dimethylated H3 K9, and an increase in total acetylated H3.

The second avenue is to replicate part of the study done in Ozdemir et al. where the MSCs were cultured with the nanofibers in a mixed 1:1:1 adipogenic:osteogenic:chondrogenic media, and then western blots were performed to determine whether the MSCs displayed an increase/decrease in adipogenic, osteogenic, and chondrogenic markers. This would confirm that the epigenetic changes observed on the MSCs are in fact connected to to the cell differentiation.

A third avenue would be to investigate the effects of different sized (200 nm to 1.5 µm) PMMA nanofibers on various epigenetic markers. More proteins could be analyzed such as, among many others, trimethylated H3 K27, methylated H4 K20, and methylated H3 K79 (all shown to have a role in transcriptional activation or silencing) (Huang et al., 2015).

A fourth avenue would be to examine the affects of alignment on the various epigenetic markers as well as differentiation. Alignment of nanofibers as well as the direction mechanical strain have both been shown to play a large role in the deposition of collagen by fibroblasts (C. H. Lee et al., 2005). Nanofiber alignment has been shown to play a role leading to increased differentiation of myoblasts and tendon stem cells (Ku, Lee, & Park, 2012) (Yin et al., 2010).

Finally, a fifth avenue would be to determine whether different nanofiber materials such as PCL, PLGA, PVA, or even silk, cause differences in the epigenetic profile of MSCs when they are placed on the nanofibers. Potentially, all of these avenues could be combined into a comprehensive study that examined the relationship between diameter, alignment, tension on the epigenetics and differentiation of stem cells. More importantly, the knowledge derived from these future studies can allow future regenerative medicine researchers to design the optimal scaffold for whatever lineage they want a cell to differentiate into.

Appendix A

PMMA Nanofiber Diameter Photos (40X)

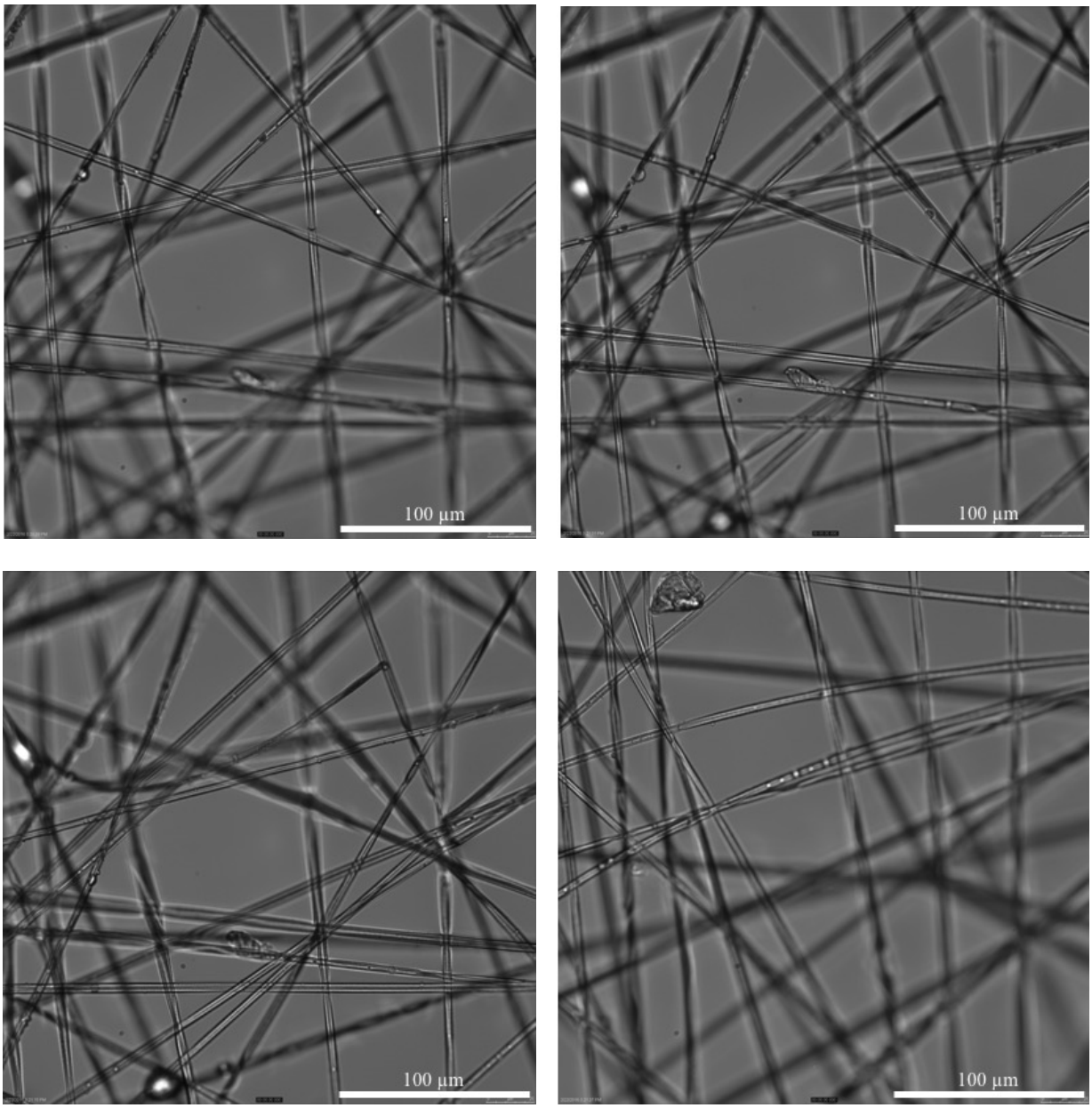

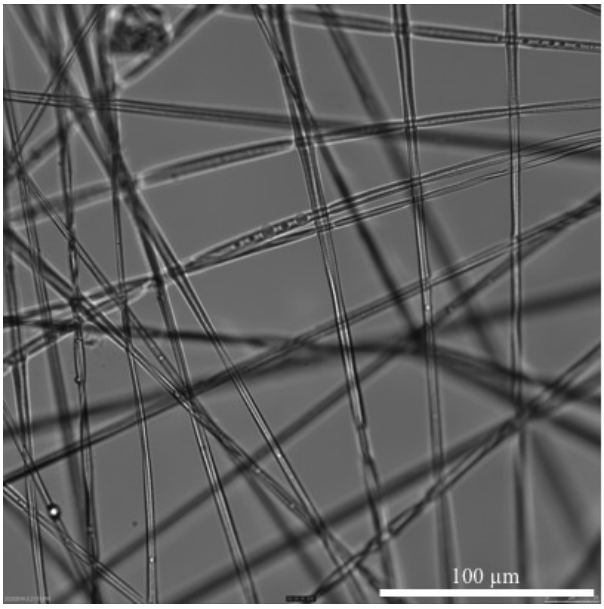
100 µm

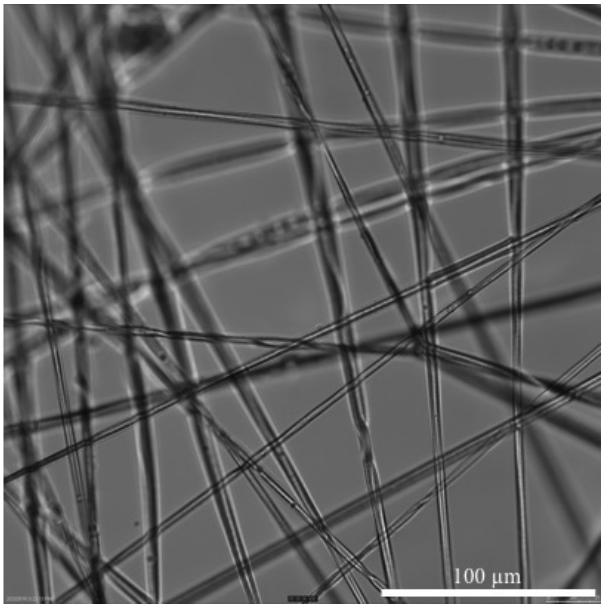
100 µm

BIBLIOGRAPHY

A “Holy Grail” Of Healing - CBS News. (n.d.). Retrieved November 15, 2015, from http://www.cbsnews.com/news/a-holy-grail-of-healing/

Atala, A., Bauer, S. B., Soker, S., Yoo, J. J., & Retik, A. B. (2006). Tissue-engineered autologous bladders for patients needing cystoplasty. *Lancet*, *367*(9518), 1241–6. doi:10.1016/S0140-6736(06)68438-9

Bell, E., Sher, S., Hull, B., Merrill, C., Rosen, S., Chamson, A., ... & Nusgens, B. (1983). The reconstitution of living skin. *Journal of investigative dermatology*, *81*.

Boutahar, N., Guignandon, A., Vico, L., & Lafage-Proust, M. H. (2004). Mechanical strain on osteoblasts activates autophosphorylation of focal adhesion kinase and proline-rich tyrosine kinase 2 tyrosine sites involved in ERK activation. *Journal of Biological Chemistry*, *279*(29), 30588-30599.

Caplan, A. I., & Dennis, J. E. (2006). Mesenchymal stem cells as trophic mediators. *Journal of Cellular Biochemistry*, *98*(5), 1076–84. doi:10.1002/jcb.20886

Carpenter, G., & Cohen, S. (1979). Epidermal growth factor. *Annual review of biochemistry*, *48*(1), 193-216.

Caruso, A. B., & Dunn, M. G. (2005). Changes in mechanical properties and cellularity during long-term culture of collagen fiber ACL reconstruction scaffolds. *Journal of Biomedical Materials Research. Part A*, *73*(4), 388–97. doi:10.1002/jbm.a.30233

Chan, B. P., & Leong, K. W. (2008). Scaffolding in tissue engineering: general approaches and tissue-specific considerations. *European Spine Journal : Official Publication of the European Spine Society, the European Spinal Deformity Society, and the European Section of the Cervical Spine Research Society*, *17 Suppl 4*, 467–79. doi:10.1007/s00586-008-0745-3

Chevalier, E., Chulia, D., Pouget, C., & Viana, M. (2008). Fabrication of porous substrates: a review of processes using pore forming agents in the biomaterial field. *Journal of pharmaceutical sciences*, *97*(3), 1135-1154.

Cyranoski, D. (2014). Japanese woman is first recipient of next-generation stem cells. *Nature*. doi:10.1038/nature.2014.15915

Dhariwala, B., Hunt, E., & Boland, T. (2004). Rapid prototyping of tissue-engineering constructs, using photopolymerizable hydrogels and stereolithography. *Tissue Engineering*, *10*(9-10), 1316–22. doi:10.1089/ten.2004.10.1316

Downing, T. L., Soto, J., Morez, C., Houssin, T., Fritz, A., Yuan, F., … Li, S. (2013a). Biophysical regulation of epigenetic state and cell reprogramming. *Nature Materials*, *12*(12), 1154–62. doi:10.1038/nmat3777

Dvir, T., Timko, B. P., Brigham, M. D., Naik, S. R., Karajanagi, S. S., Levy, O., ... & Kohane, D. S. (2011). Nanowired three-dimensional cardiac patches. *Nature nanotechnology*, *6*(11), 720-725.

Engelmayr, G. C., Cheng, M., Bettinger, C. J., Borenstein, J. T., Langer, R., & Freed, L. E. (2008). Accordion-like honeycombs for tissue engineering of cardiac anisotropy. *Nature Materials*, *7*(12), 1003–10. doi:10.1038/nmat2316

Engler, A. J., Sen, S., Sweeney, H. L., & Discher, D. E. (2006). Matrix elasticity directs stem cell lineage specification. *Cell*, *126*(4), 677–89. doi:10.1016/j.cell.2006.06.044

Gaydos, L., Wang, W., & Strome, S. (2014). H3K27me and PRC2 transmit a memory of repression across generations and during development. *Science*. Retrieved from http://science.sciencemag.org/content/345/6203/1515.short

Hersel, U., Dahmen, C., & Kessler, H. (2003). RGD modified polymers: biomaterials for stimulated cell adhesion and beyond. *Biomaterials*, *24*(24), 4385–4415. doi:10.1016/S0142-9612(03)00343-0

Hirai, J., Kanda, K., Oka, T., & Matsuda, T. (1994). Highly oriented, tubular hybrid vascular tissue for a low pressure circulatory system. *ASAIO journal*,*40*(3), M383-M388.

Hirai, J., & Matsuda, T. (1996). Venous reconstruction using hybrid vascular tissue composed of vascular cells and collagen: tissue regeneration process.*Cell transplantation*, *5*(1), 93-105.

Hou, P., Li, Y., Zhang, X., Liu, C., Guan, J., Li, H., ... & Ge, J. (2013). Pluripotent stem cells induced from mouse somatic cells by small-molecule compounds. *Science*, *341*(6146), 651-654.

Huang, B., Li, G., & Jiang, X. H. (2015). Fate determination in mesenchymal stem cells: a perspective from histone-modifying enzymes. *Stem Cell Research & Therapy*, *6*(1), 35. doi:10.1186/s13287-015-0018-0

Huang, Z.-M., Zhang, Y.-Z., Kotaki, M., & Ramakrishna, S. (2003). A review on polymer nanofibers by electrospinning and their applications in nanocomposites. *Composites Science and Technology*, *63*(15), 2223–2253. doi:10.1016/S0266-3538(03)00178-7

Jaiswal, D., & Brown, J. L. (2012). Nanofiber diameter-dependent MAPK activity in osteoblasts. *Journal of Biomedical Materials Research. Part A*, *100*(11), 2921–8. doi:10.1002/jbm.a.34234

Kai, D., Jin, G., Prabhakaran, M. P., & Ramakrishna, S. (2013). Electrospun synthetic and natural nanofibers for regenerative medicine and stem cells. *Biotechnology Journal*, *8*(1), 59–72. doi:10.1002/biot.201200249

Kakisis, J. D., Liapis, C. D., Breuer, C., & Sumpio, B. E. (2005). Artificial blood vessel: The Holy Grail of peripheral vascular surgery. *Journal of Vascular Surgery*, *41*(2), 349–354. doi:10.1016/j.jvs.2004.12.026

Kolf, C. M., Cho, E., & Tuan, R. S. (2007). Biology of adult mesenchymal stem cells: regulation of niche, self-renewal and differentiation. *Arthritis res ther*, *9*(1), 204.

Ku, S. H., Lee, S. H., & Park, C. B. (2012). Synergic effects of nanofiber alignment and electroactivity on myoblast differentiation. *Biomaterials*, *33*(26), 6098–104. doi:10.1016/j.biomaterials.2012.05.018

Lee, C. H., Shin, H. J., Cho, I. H., Kang, Y.-M., Kim, I. A., Park, K.-D., & Shin, J.-W. (2005). Nanofiber alignment and direction of mechanical strain affect the ECM production of human ACL fibroblast. *Biomaterials*, *26*(11), 1261–70. doi:10.1016/j.biomaterials.2004.04.037

Lee, J., Green, M., & Amiel, D. (1995). Synergistic effect of growth factors on cell outgrowth from explants of rabbit anterior cruciate and medial collateral ligaments. *Journal of Orthopaedic Research*. Retrieved from http://onlinelibrary.wiley.com/doi/10.1002/jor.1100130318/pdf

Linkhart, T. A., Mohan, S., & Baylink, D. J. (1996). Growth factors for bone growth and repair: IGF, TGFβ and BMP. *Bone*, *19*(1), S1–S12. doi:10.1016/S8756-3282(96)00138-X

Macchiarini, P., Jungebluth, P., Go, T., Asnaghi, M. A., Rees, L. E., Cogan, T. A., … Birchall, M. A. (2008). Clinical transplantation of a tissue-engineered airway. *Lancet*, *372*(9655), 2023–30. doi:10.1016/S0140-6736(08)61598-6

Margueron, R., & Reinberg, D. (2010). Chromatin structure and the inheritance of epigenetic information. *Nature Reviews. Genetics*, *11*(4), 285–96. doi:10.1038/nrg2752

Martin, G. R. (1981). Isolation of a pluripotent cell line from early mouse embryos cultured in medium conditioned by teratocarcinoma stem cells.*Proceedings of the National Academy of Sciences*, *78*(12), 7634-7638.

Mascarenhas, R., & MacDonald, P. B. (2008). Anterior cruciate ligament reconstruction: a look at prosthetics-past, present and possible future. *McGill Journal of Medicine*, *11*(1), 29.

McBeath, R., Pirone, D. M., Nelson, C. M., Bhadriraju, K., & Chen, C. S. (2004). Cell Shape, Cytoskeletal Tension, and RhoA Regulate Stem Cell Lineage Commitment. *Developmental Cell*, *6*(4), 483–495. doi:10.1016/S1534-5807(04)00075-9

Michalopoulos, G. K. (2007). Liver regeneration. *Journal of Cellular Physiology*, *213*(2), 286–300. doi:10.1002/jcp.21172

Morrison, J. I., Lööf, S., He, P., & Simon, A. (2006). Salamander limb regeneration involves the activation of a multipotent skeletal muscle satellite cell population. *The Journal of Cell Biology*, *172*(3), 433–40. doi:10.1083/jcb.200509011

Murray, M. M., Rice, K., Wright, R. J., & Spector, M. (2003). The effect of selected growth factors on human anterior cruciate ligament cell interactions with a three-dimensional collagen-GAG scaffold. *Journal of orthopaedic research*, *21*(2), 238-244.

Nerurkar, N. L., Baker, B. M., Sen, S., Wible, E. E., Elliott, D. M., & Mauck, R. L. (2009). Nanofibrous biologic laminates replicate the form and function of the annulus fibrosus. *Nature Materials*, *8*(12), 986–92. doi:10.1038/nmat2558

Osteogenesis. (n.d.). Retrieved March 22, 2016, from http://www.york.ac.uk/res/bonefromblood/background/osteogenesis.html

Ott, H. C., Matthiesen, T. S., Goh, S.-K., Black, L. D., Kren, S. M., Netoff, T. I., & Taylor, D. A. (2008). Perfusion-decellularized matrix: using nature's platform to engineer a bioartificial heart. *Nature Medicine*, *14*(2), 213–21. doi:10.1038/nm1684

Ozdemir, T., Higgins, A. M., & Brown, J. L. (2015). Molecular mechanisms orchestrating the stem cell response to translational scaffolds. *Conference Proceedings : ... Annual International Conference of the IEEE Engineering in Medicine and Biology Society. IEEE Engineering in Medicine and Biology Society. Annual Conference*, *2015*, 1749–52. doi:10.1109/EMBC.2015.7318716

Reneker, D. H., & Chun, I. (1996). Nanometre diameter fibres of polymer, produced by electrospinning. *Nanotechnology*, *7*(3), 216.

Salasznyk, R. M., Klees, R. F., Williams, W. A., Boskey, A., & Plopper, G. E. (2007). Focal adhesion kinase signaling pathways regulate the osteogenic differentiation of human mesenchymal stem cells. *Experimental Cell Research*, *313*(1), 22–37. doi:10.1016/j.yexcr.2006.09.013

Schiffman, J. D., & Schauer, C. L. (2008). A Review: Electrospinning of Biopolymer Nanofibers and their Applications. *Polymer Reviews*, *48*(2), 317–352. doi:10.1080/15583720802022182

Sen, M. K., & Miclau, T. (2007). Autologous iliac crest bone graft: should it still be the gold standard for treating nonunions? *Injury*, *38 Suppl 1*, S75–80. doi:10.1016/j.injury.2007.02.012

Shum-Tim, D., Stock, U., Hrkach, J., Shinoka, T., Lien, J., Moses, M. A., ... & Langer, R. (1999). Tissue engineering of autologous aorta using a new biodegradable polymer. *The Annals of thoracic surgery*, *68*(6), 2298-2304.

Takahashi, K., & Yamanaka, S. (2006). Induction of pluripotent stem cells from mouse embryonic and adult fibroblast cultures by defined factors. *Cell*, *126*(4), 663–76. doi:10.1016/j.cell.2006.07.024

Teo, W. E., & Ramakrishna, S. (2006). A review on electrospinning design and nanofibre assemblies. *Nanotechnology*, *17*(14), R89–R106. doi:10.1088/0957-4484/17/14/R01

Vacanti, J. P., Morse, M. A., Saltzman, W. M., Domb, A. J., Perez-Atayde, A., & Langer, R. (1988). Selective cell transplantation using bioabsorbable artificial polymers as matrices. *Journal of Pediatric Surgery*, *23*(1), 3–9. doi:10.1016/S0022-3468(88)80529-3

Vacanti, J. P., Morse, M. A., Saltzman, W. M., Domb, A. J., Perez-Atayde, A., & Langer, R. (1988). Selective cell transplantation using bioabsorbable artificial polymers as matrices. *Journal of pediatric surgery*, *23*(1), 3-9.

Watanabe, M., Shin'oka, T., Tohyama, S., Hibino, N., Konuma, T., Matsumura, G., … Morita, S. (2001). Tissue-engineered vascular autograft: inferior vena cava replacement in a dog model. *Tissue Engineering*, *7*(4), 429–39. doi:10.1089/10763270152436481

Wigler, M., Levy, D., & Perucho, M. (1981). The somatic replication of DNA methylation. *Cell*, *24*(1), 33-40.

Yin, Z., Chen, X., Chen, J. L., Shen, W. L., Hieu Nguyen, T. M., Gao, L., & Ouyang, H. W. (2010). The regulation of tendon stem cell differentiation by the alignment of nanofibers. *Biomaterials*, *31*(8), 2163–75. doi:10.1016/j.biomaterials.2009.11.083

Zaidel-Bar, R., & Geiger, B. (2010). The switchable integrin adhesome. *Journal of cell science*, *123*(9), 1385-1388.

ACADEMIC VITA

Matthew Swatski

405 Woodside Avenue, Narberth PA 19072− 610-256-0189 – mds5532@psu.edu

Education	**Pennsylvania State University** College of Engineering, Schreyer Honors College Major: Biomedical Engineering, Chemical Option	**Fall 2012-Present**
Research Experience	**Research in Musculoskeletal Regeneration Lab** I am working in Dr. Justin Brown's Regenerative Medicine Lab	**Fall 2013-Present**
	Weis Center for Research Summer Undergraduate Research Program I investigated the role that the enzyme COX-2 plays in down-regulating the kinetochore and centromere proteins in prostate cancer cells. I was third author on a journal paper in *The Prostate* (See **Publication**)	**Summer 2013**
Publication	**Peer-Reviewed Journal Article** Bieniek, J., Childress, C., Swatski, M. D., & Yang, W. (2014). COX-2 inhibitors arrest prostate cancer cell cycle progression by down-	**2014**
Technical Skills	HPLC, MS, ELISA, SDS-PAGE, UV/Vis spectroscopy, fluorescence staining, RT-PCR, DNA gel electrophoresis, basic cell culture techniques, IR, electrospinning, 3D printing, and soldering	**Fall 2012-Present**
Relevant Coursework	Tissue Engineering/Regenerative Medicine, Inorganic Chemistry, Organic Chemistry, Biochemistry, Cell Biology, Mass Transport	**Fall 2012-Present**
Relevant Skills	Microsoft Office, MATLAB, C++	**Fall 2012-Present**